

國立臺灣大學醫學院免疫學研究所

碩士論文

Graduate Institute of Immunology

College of Medicine

National Taiwan University

Master Thesis



探討介白質-15 異構蛋白對於介白質-15 調節訊息傳遞、T 細胞存活及與介白質-15 受器 α 結合的影響

Effects of an alternatively spliced IL-15 isoform on IL-15-mediated signaling, T cell survival and IL-15R α binding

張毅軒

Yi-Hsuan Chang

指導教授：顧家綺 博士

Advisor: Chia-Chi Ku, Ph. D.

中華民國一零五年七月

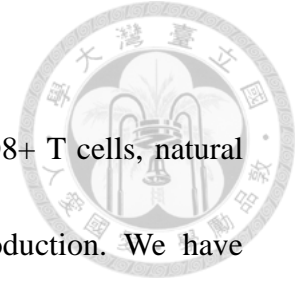
July, 2016

誌謝

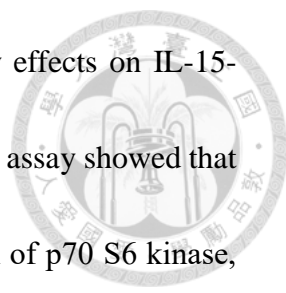


騎著腳踏車沿著仁愛路劃過大安森林公園，返家路上想了許久，依舊無法決定誌謝順序，免疫所的這兩年間，沒有身邊這些人的陪伴就無法成就今日的我與背包中百頁的論文，即使只是一句問候、一個微笑甚至於只是在走廊上相視而過，這些日常都是身處艱困時能夠支持著我的寄託。雖然與每個人的相遇、認識都是重要的，但若是沒有家人們的幫助，或許我連免疫所都進不成，我將最誠摯且最盛大的感謝獻給他們，謝謝願意當我的後盾，支持我這碩士兩年花了超過五十萬的兒子，同時也包容我鮮少回家或是打電話問候，我對他們付出的極少，卻無怨無悔的將一切奉獻給我，僅獻上這本論文代表我沒有白費你們的辛勞。在學習免疫學的殿堂上，我由衷感謝指導教授，顧家綺老師對我的栽培，回想大學時修習基免時已對老師認真教學的風格很有印象，錄取後，著實地接受老師的教誨以學會科學研究的方法，同時也感謝口試委員孔祥智老師、李建國老師以及徐立中老師的不辭辛勞，給予許多建議幫助我完成論文。謝謝同實驗室的奕源學長教我實驗和簡筠學姊引領我適應實驗室生活，最感謝林宇瑞這兩年的陪伴讓我能夠歡樂地待在實驗室、Austin 幫我修訂論文，還有于主念學弟對於學長姐的關懷。也謝謝同屆的伯翰、彥霏、承訓、婉瑜、宜臻、鈺舒、僑莉、卉玲、妍璋、家琳、京育、怡君、牧昀及仕宸，何其榮幸能夠一同學習、出遊和分享彼此的血淚，能與你們是一班真是太好了。五樓的許、朱、李、繆及伍家實驗室的其他學長姊弟妹們，謝謝你們容忍我常去閒聊，特別是許家比鄰顧家更常受到我的叨擾。也謝謝師丈和林挺輝學長在 FPLC 方面幫助我許多和李明學老師實驗室也提供很多蛋白質純化協助。其他族繁不及備載的人們，請原諒因篇幅關係沒有提及你們，在過去兩年間，跌跌撞撞前進的我，若是沒有你們我也無法堅持至今。完稿的現在，仍舊回味那段痛苦但溫暖的時光，但未來依然一直來，我不知道羽翼是否以豐滿，但相信經過這兩年的薰陶，我能夠獨自面對接下來颳起的任何一場颶風。

Abstract



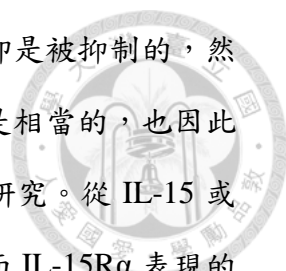
IL-15 mediates the proliferation and survival of memory CD8⁺ T cells, natural killer (NK) and NKT cells as well as enhancing cytokine production. We have previously shown that an alternatively spliced IL-15 isoform that has partial deletion in exon 7 of the IL-15 gene (IL-15 Δ E7) failed to activate phosphorylation of STAT5 and blocked transcription of anti-apoptotic gene bcl-2 in an IL-2/IL-15 dependent T cell line (HT-2 cells). In this thesis, I have successfully generated recombinant IL-15 Δ E7 and IL-15 proteins from yeast expression system and confirmed by Fast Protein Liquid Chromatography (FPLC) and Western Blot analyses. To further investigate the effects of IL-15 Δ E7 on cell survival, IL-15 Δ E7-treated or IL-15-treated HT-2 cells were examined for cell apoptosis by detecting the expression of phosphatidylserine (PS) on the plasma membrane and DNA fragmentation by flow cytometric analysis. HT-2 cells were proliferative and survived in IL-15 culture. However, high percentage of cells underwent apoptosis at 12 h and all cells died at 24 h in IL-15 Δ E7-treated HT-2 cells. The patterns were similar to cytokine-deprived control cells. Pretreatment of HT-2 cells with IL-15 Δ E7 followed by IL-15 treatment or co-treatment of the cells with a mixture of IL-15 and IL-15 Δ E7 did not blocked IL-15-mediated cell survival and proliferation. High concentration of IL-15 Δ E7 treatment did not promote cell death in IL-15 treated cells. These experiments demonstrated that while IL-15 Δ E7 failed to support HT-2 cell



survival, exogenous addition of IL-15ΔE7 did not exert inhibitory effects on IL-15-mediated cell proliferation. Signalosome analysis by Micro-Western assay showed that IL-15ΔE7 treatment resulted in increased levels of phosphorylation of p70 S6 kinase, SrcY⁴¹⁶, SrcY⁵²⁷, Syk and GSK3 compared with those in IL-15 treated cells. Increased protein level of IκB was also observed. Further analysis of the protein phosphorylation in MAPK pathways and SrcY⁴¹⁶ by conventional Western blot confirmed that IL-15ΔE7 failed to phosphorylate ERK but enhanced phosphorylation of JNK, P38 and SrcY⁴¹⁶. IL-15 induced phosphorylation of IKK was suppressed in IL-15ΔE7 treated cells. Since the phosphorylation levels of p65 were comparable in IL-15-treated and IL-15ΔE7-treated cells, the role of IL-15ΔE7 in NF-κB signaling pathways requires further investigation. Analysis of the binding of IL-15 or IL-15ΔE7 to IL-15Rα and the effects on the surface expression of IL-15Rα after ligand binding demonstrated that IL-15ΔE7 bound to IL-15Rα with very low affinity compared with IL-15. IL-15 triggered downregulation of surface expression of IL-15Rα was less significant in IL-15ΔE7-treated cells. Since *trans*-presentation of IL-15 by IL-15Rα on myeloid cells is known as an important mechanism for developing effector functions of T cells and NK cells, the role for IL-15ΔE7 in regulating IL-15 function via *trans*-presentation is worth of further investigation.

摘要

介白質-15 (Interleukin-15, IL-15) 是一個多效型的細胞激素，能夠調節記憶性 CD8 T 細胞 (Memory CD8⁺ T cell)、自然殺手細胞 (Natural killer cell, NK cell) 及自然殺手 T 細胞 (Natural killer T cell, NKT cell) 的複製和存活，同時也能夠促進其他細胞激素的表現。本實驗室過去的研究中發現，一種缺少了部分的第七外顯子的 IL-15 選擇性剪接異構體，(以下簡稱 IL-15ΔE7)，無法促進 IL-2 和 IL-15 依賴性細胞 HT-2 細胞的 STAT5 的磷酸化以及抗細胞凋亡基因 *bcl-2* 的轉錄。在本論文研究，我成功建立酵母菌蛋白表現與純化系統製造重組 IL-15 以及 IL-15ΔE7 二種蛋白，並且經過西方墨點法及快速液態層析儀 (Fast Protein Liquid Chromatography, FPLC) 確認該蛋白的活性與生化特性。為了更進一步研究 IL-15ΔE7 對於細胞存活的影响，利用了流式細胞儀分析分別經過 IL-15 以及 IL-15ΔE7 處理後的 HT-2 細胞，藉以偵測細胞膜上磷脂絲胺酸 (phosphatidylserine, PS) 外翻及 DNA 斷裂的程度以檢驗細胞凋亡的情況。在以 IL-15 培養的情況下，大部分 HT-2 細胞存活並具有增殖性；然而，有很高比例的 IL-15ΔE7 處理過後的 HT-2 細胞在第 12 小時進行細胞凋亡，而全部的細胞在第 24 小時死亡，這樣的情況與去除細胞激素培養的控制組細胞類似。以 IL-15ΔE7 預處理接著以 IL-15 處理或者同時以 IL-15ΔE7 和 IL-15 處理的 HT-2 細胞，這兩種處理方式都不會抑制 IL-15 促進細胞存活與增殖的作用；此外，高濃度的 IL-15ΔE7 刺激也不會引起 IL-15 培養的細胞死亡。這些實驗闡述了雖然 IL-15ΔE7 無法維持 HT-2 細胞的存活，但是外部添加 IL-15ΔE7 也無法抑制 IL-15 調節的細胞增生。利用 Micro-Western 進行訊號體 (Signalosome) 分析的實驗指出，IL-15ΔE7 能夠相較於 IL-15 引起更多的 P70 S6 kinase、SrcY⁴¹⁶、SrcY⁵²⁷、Syk 以及 GSK3 的磷酸化，同時我們也觀察到更多 IκB 的蛋白質累積；更進一步地，我們使用傳統的西方墨點法以檢驗 MAPK 和 SrcY⁴¹⁶ 的訊息傳導並確認了 IL-15ΔE7 無法造成 ERK 的磷酸化，卻能夠造成更多的 JNK、P38 和 SrcY⁴¹⁶ 的磷酸化，我



們也發現 IL-15 引起的 IKK 磷酸化在 IL-15 Δ E7 刺激的細胞中卻是被抑制的，然而，P65 的磷酸化程度在 IL-15 Δ E7 和 IL-15 刺激的細胞中卻是相當的，也因此 IL-15 Δ E7 在 NF- κ B 訊息傳遞當中所扮演的角色需要更深入的研究。從 IL-15 或者 IL-15 Δ E7 結合至 IL-15R α 的情況分析及結合後對於細胞表面 IL-15R α 表現的影響結果當中指出，相對 IL-15 而言，IL-15 Δ E7 以非常低的親和力結合上 IL-15R α ；同時，IL-15 所引起的細胞表面 IL-15R α 的表現量下降，在 IL-15 Δ E7 處理的細胞則不顯著。已知藉由非淋巴性白血球轉位呈現 (*trans*-presentation) IL-15 至 T 細胞和 NK 細胞是對於這兩類細胞能夠發展出活化後功能的重要機制；因此，未來的實驗應該加強探討 IL-15 Δ E7 如何藉由調控轉位呈現得以調節 IL-15 的功能。

Table of Contents



誌謝.....	i
Abstract.....	ii
摘要.....	iv
Table of Contents	vi
List of Figures.....	ix
Chapter I. Introduction.....	1
Part I. Interleukin-15 (IL-15).....	1
1. Characteristics	1
2. Functions	1
3. <i>Trans</i> -presentation.....	3
Part II. The interaction of IL-15 with IL-15R α , IL-2/IL-15R β and γ_c	4
Part III. Signal transduction through IL-2/IL-15R β and γ_c	6
Part IV. NF- κ B signaling pathway	6
Part V. Hypothesis of IL-15 Δ E7 structure	7
Part VI. <i>Pichia</i> expression system.....	8
Chapter II. Aims of the Study	9
1. Establishment of Yeast protein expression system to generate recombinant IL-15 Δ E7 and IL-15 protein.....	9
2. Functions of IL-15 Δ E7 on cell proliferation and survival.....	10
3. Signalosome analysis of IL-15 Δ E7 induced signaling activation in HT-2 cells	10
4. Effects of IL-15 Δ E7 on the cell surface expression of IL-15R α	11
Chapter III. Materials and Methods.....	12
Part I. Methods	12
1. Cell lines and cell culture	12

2. Construction of the X-33 strain expressing mouse IL-15 and IL-15ΔE7	12
2.1 Construction of pPICZαA-mIL-15(FLAG) and pPICZαA-mIL-15ΔE7(FLAG)	12
2.2 Transformation of pPICZαA-mIL-15ΔE7(FLAG) and pPICZαA-mIL-15 (FLAG) into the X-33 strain	15
3. Expression and purification of yeast recombinant IL-15 or IL-15ΔE7	15
3.1 Induction of yeast recombinant IL-15 or IL-15ΔE7	15
3.2 Purification of yeast recombinant IL-15 or IL-15ΔE7	16
4. Deglycosylation analysis of yeast recombinant IL-15 and IL-15ΔE7	16
5. Coomassie blue staining of yeast recombinant IL-15 and IL-15ΔE7	17
6. Western blotting	17
7. IL-15 and IL-15ΔE7 biological assay using HT-2 cells	18
8. Flow cytometry analysis	19
8.1 Apoptosis assay	19
8.2 Immunodetection of expression of surface IL-15Rα and surface attached IL-15 isoforms on IL-15Rα-COS-7 cells	19
Part II. Materials	20
1. List of antibodies	20
2. List of primers	22
3. Solutions	22
Chapter IV. Results	28
1. Expression and purification of Yeast recombinant IL-15ΔE7 and IL-15	28
1.1 Strategy of constructing yeast plasmid expressing IL-15ΔE7 or IL-15	28
1.2 Construction of recombinant IL-15ΔE7 and IL-15 expressing X33 strain	29
1.3 Expression and characterization of yeast recombinant IL-15ΔE7 and IL-15	30
1.4 FPLC analysis of yeast recombinant IL-15ΔE7 and IL-15	31
1.5 Function analysis of yeast recombinant IL-15ΔE7 and IL-15	32
2. Apoptosis and proliferation assay of IL-15ΔE7 functions	33
2.1 Apoptosis assays of IL-15ΔE7-treated HT-2 cells	33
2.2 IL-15ΔE7 failed to support HT-2 cell survival	34

2.3 IL-15ΔE7 failed to inhibit IL-15 mediated cell survival.	35
2.4 IL-15ΔE7 fails to inhibit IL-15 mediated cell proliferation.	36
3. Signalosome analysis of IL-15ΔE7 induced signaling activation in HT-2 cells	37
3.1 IL-15ΔE7 activated alternative signaling pathways different from IL-15 mediated responses.	38
3.2 IL-15ΔE7 induced JNK, P38 and SrcY ⁴¹⁶ phosphorylation but not ERK phosphorylation.	39
3.3 IL-15ΔE7 failed to induce phosphorylation of IKK but enhances phosphorylation of P65.....	39
4. Effects of IL-15ΔE7 on the cell surface expression of IL-15Rα	40
4.1 The reasons of investigating the role of IL-15ΔE7 to <i>trans</i> -presentation	40
4.2 IL-15ΔE7 bond to IL-15Rα with an extremely low affinity.....	41
4.3 Time course analysis of surface IL-15Rα downregulation induced by IL-15ΔE7	42
4.4 IL-15ΔE7 induced surface IL-15Rα downregulation in the overnight culture.....	44
Chapter V. Discussion	45
1. Establishment of <i>Pichia</i> expression system to generate recombinant IL-15 and IL-15ΔE7	46
2. The regulatory functions of IL-15ΔE7 on HT-2 cells	48
3. Analysis of IL-15ΔE7 mediated signaling pathways	49
4. The differences in affinity and regulation of surface IL-15Rα between IL-15 and IL-15ΔE7	51
5. The connection between <i>in vitro</i> experiments and P191 mouse phenotypes	53
References	57
Figures.....	64
Appendix.....	89

List of Figures



- Figure 1. Generation of recombinant IL-15 and IL-15 Δ E7 from *Pichia* yeast expression system
- Figure 2. Verification of IL-15 and IL-15 Δ E7 construct using restriction enzyme digestion and colony PCR
- Figure 3. Genotyping of IL-15 and IL-15 Δ E7 transformed X-33 strain
- Figure 4. Western blot analysis of purified yeast recombinant IL-15 and IL-15 Δ E7
- Figure 5. Western blot analysis of deglycosylated IL-15 and IL-15 Δ E7
- Figure 6. FPLC analysis of recombinant IL-15 and IL-15 Δ E7 proteins prepared from yeast expression system
- Figure 7. The cell viability and the phosphorylation of STAT5 in HT-2 cells after treated with yeast recombinant IL-15 and IL-15 Δ E7
- Figure 8. Induction of cell apoptosis in HT-2 cells by camptothecin treatment.
- Figure 9. IL-15 Δ E7 did not enhance apoptosis of cytokine-deprived HT-2 cells.
- Figure 10. IL-15 Δ E7 did not affect IL-15 functions of cell survival maintenance and apoptosis inhibition.
- Figure 11. Exogenous addition of IL-15 Δ E7 at all doses does not block IL-15-mediated HT-2 cell proliferation.

Figure 12. Signalosome profiles in IL-15 Δ E7-treated HT-2 cells by Micro-western analysis



Figure 13. Activation of Src and MAPK pathway by IL-15 Δ E7

Figure 14. IL-15 Δ E7 treatment suppressed IKK $\alpha\beta$ phosphorylation but enhanced P65 phosphorylation compared to IL-15 treatment.

Figure 15. Dose effects of IL-15 or IL-15 Δ E7 on the surface expression of IL-15 or IL-15R α in IL-15R α -COS-7 cells

Figure 16. Temporal expression of IL-15R α in IL-15R α -COS-7 cells after treated with IL-15 or IL-15 Δ E7

Figure 17. Surface expression of IL-15R α in IL-15R α -COS-7 cells after treated with IL-15 or IL-15 Δ E7 overnight

Chapter I. Introduction



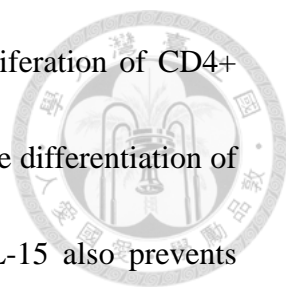
Part I. Interleukin-15 (IL-15)

1. Characteristics

IL-15 is the member of IL-2 cytokine family. The IL-15 gene (>34 kb) is comprised of eight introns and nine exons and located on the chromosome 4 in human and the chromosome 8 in mouse, respectively (Fehniger and Caligiuri 2001). The 14-15 kDa IL-15 protein is encoded by exons 5 to 8 of the IL-15 gene and forms a 4- α helical bundle structure. The biological functions of IL-15 are mediated by interaction with a heterotrimeric receptor consisting of an unique IL-15R α and the shared β and the common γ chains of IL-2 receptor (IL-2/15R $\beta\gamma_c$) (Waldmann 2006).

2. Functions

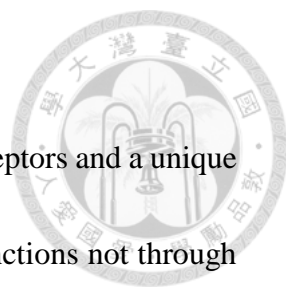
The function of IL-15 is pleiotropic. IL-15 is known to mediate proliferation and survival of memory CD8⁺ T cells, natural killer (NK) and NKT cells (Perera, Lichy et al. 2012). IL-15 also promotes production of IL-12 from dendritic cells (Ohteki, Suzue et al. 2001). IL-15 also promotes production of IL-12 from dendritic cells (Ohteki, Suzue et al. 2001), regulating the differentiation of T_H1 cell (Hsieh, Macatonia et al. 1993, Ohteki, Suzue et al. 2001). In addition, IL-15 has the ability to induce intestinal DC to secrete IL-23, which enhances T_H17 cell differentiation (DePaolo, Abadie et al. 2011,



Pandiyan, Yang et al. 2012). IL-15 is also shown to enhance proliferation of CD4⁺ regulatory T (T_{Reg}) cells (Imamichi, Sereti et al. 2008) but blocks the differentiation of peripherally derived T_{Reg} cells (DePaolo, Abadie et al. 2011). IL-15 also prevents FOXP3⁺ T_{Reg} cells from exerting their inhibitory functions on effector T cells such as inhibition of CD8 effector T cell proliferation and prevention of IFN γ production by CD4 helper T cell through activation of PI3K signaling pathways in CD4 and CD8 effector T cells (Ben Ahmed, Belhadj Hmida et al. 2009).

As a cell growth promoting cytokine, IL-15 not only promotes immune cell proliferation but also maintains non-immune cell survival. For example, keratinocytes which are able to secrete IL-15 and express IL-15R $\alpha\beta\gamma$ on their cell surface are protected by IL-15 signaling from anti-Fas and methylcellulose induced apoptosis *in vitro* (Ruckert, Asadullah et al. 2000). In addition, IL-15 also prevents T cell-dependent apoptosis and anti-Fas or actinomycin D induced cell death in kidney epithelium cells from (Shinozaki, Hirahashi et al. 2002). Moreover, endogenous IL-15 has been shown to reduce mucosal damage by preventing intestinal epithelium cell death in chronic colitis (Obermeier, Hausmann et al. 2006). These evidences have suggested a pro-survival role for IL-15.

3. *Trans*-presentation



IL-15 signaling is mediated by IL-2/IL-15R β and γ_c of IL-2 receptors and a unique IL-15R α . Although IL-15 shares two receptors with IL-2, IL-15 functions not through *cis*-presentation but mainly in a cell-contact dependent manner through *trans*-presentation demonstrated both *in vitro* and *in vivo* (Jabri and Abadie 2015). When tissue undergoes stress, antigen presenting cells and non-haematopoietic tissue cells such as epithelial cells or stromal cells produce IL-15 assembled into the IL-15-IL-15R α complex in the endoplasmic reticulum. IL-15-IL-15R α is then sent to cell surface and presented *in trans* to responder cells such as T cells and NK cells expressing the heterodimer of IL-2/IL-15R β and γ_c (Jabri and Abadie 2015). When antigen presenting cells or tissue cells present antigens to effector T cells, the IL-15-IL-15R α complex is also *trans*-presented and serves as a co-stimulatory signal to promote T cell survival. *Trans*-presentation of IL-15-IL-15R α complex by antigen presenting cells is found to increase TCR mediated cytolytic functions and induce NK receptors enabling CTL to kill tissue cells of infection or stress through recognition of danger signals such as non-classical MHC molecules when the expression of MHC Class I is downregulated (Dann, Wang et al. 2005, Rausch, Hessmann et al. 2006, Jabri and Abadie 2015). Since tissue distress functions as the first messenger to *trans*-present IL-15 on the cell surface, IL-15 is able to achieve high concentration levels locally and presented to responder cells

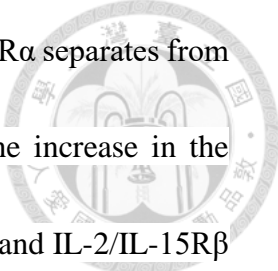
compared to IL-2 (Dubois, Mariner et al. 2002, Burkett, Koka et al. 2003).



Part II. The interaction of IL-15 with IL-15R α , IL-2/IL-15R β and γ_c

IL-15 is a four α -helical bundle protein. The production and secretion of IL-15 requires its co-expression and association with IL-15R α in the same cells under physiological condition (Schluns, Kieper et al. 2000, Koka, Burkett et al. 2003, Burkett, Koka et al. 2004, Sandau, Schluns et al. 2004, Chertova, Bergamaschi et al. 2013). It is suggested that the association constant for IL-15 and IL-15R α complex is about 10^{11} M^{-1} (Giri, Kumaki et al. 1995) in the endoplasmic reticulum. After forming the stable complex in the endoplasmic reticulum, the heterodimeric IL-15-IL-15R α complex is transported to the cell surface (Bergamaschi, Rosati et al. 2008, Bergamaschi, Jalah et al. 2009, Chertova, Bergamaschi et al. 2013). Soluble IL-15-IL-15R α complex is able to be released to the serum from the cell surface after cleaved by protease (Bergamaschi, Rosati et al. 2008).

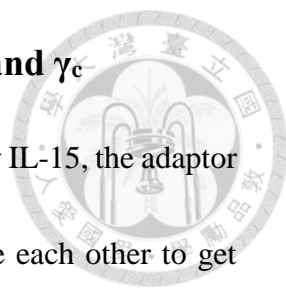
Although soluble IL-15 alone is also able to interact with IL-2/IL-15R β and γ_c with intermediate affinity ($K_a \sim 10^9 \text{ M}^{-1}$) (Lodolce, Burkett et al. 2002), interaction of IL-15-IL-15R α heterodimer with IL-2/IL-15R β and γ_c forms IL-15-IL15R $\alpha\beta\gamma_c$ quaternary complex with high affinity ($K_a \sim 10^{11} \text{ M}^{-1}$) (Stonier and Schluns 2010). IL-15 binds to IL-2/IL-15R β and γ_c . The crystal structure of IL-15-IL-15R $\alpha\beta\gamma_c$ quaternary



complexes reveals that IL-15 contacts IL-2/IL-15R β and γ_c but IL-15R α separates from IL-2/IL-15R β at least with a distance of 15 Å, suggesting that the increase in the binding affinity by ~150 folds between IL-15-IL-15R α heterodimer and IL-2/IL-15R β greatly reduces the conformational freedom of the loops of single chain IL-15 (Ring, Lin et al. 2012, Chertova, Bergamaschi et al. 2013).

The four helices of IL-15 are named helix A to D from N terminus to C terminus. IL-15 interacts with IL-2/IL-15R β using helices A and C, yielding the helices A and D and loop A-B to contact γ_c (Ring, Lin et al. 2012). The main mechanism of IL-15 interaction with IL-2/IL-15R β is not driven by conformational alternation. Instead, the receptor seems to have a rigid interface enable for the formation of many high affinity non-covalent side chains such as Van der waals forces, hydrogen bonds and ionic bonds with IL-15 (Ring, Lin et al. 2012). Unlike the highly polar and specific side-chain contacts in the interface of IL-15-IL-2/IL-15R β , IL-15 interacts with γ_c through a chemically “featureless” interface.. The strategy of IL-15 docking to γ_c is similar with those of IL-2 and IL-4, which illustrates the cross-reactivity properties of γ_c degenerative cytokine-binding surface enable to engage all members of the γ_c cytokine family (Ring, Lin et al. 2012). When IL-15-IL-15R $\alpha\beta\gamma$ quaternary complexes is formed, cytosolic parts of IL-2/IL-15R β and γ_c approach each other proximately, which induces downstream signaling molecules activation followed by gene expression.

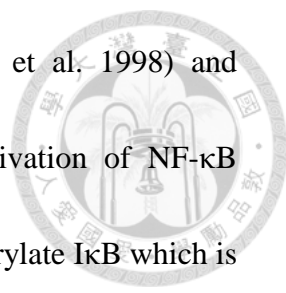
Part III. Signal transduction through IL-2/IL-15R β and γ_c



When heterodimerization of IL-2/IL-15R β and γ_c is triggered by IL-15, the adaptor protein JAK1 on IL-2/IL-15R β and JAK3 on γ_c transphosphorylate each other to get full activation of kinase activity (Haan, Rolvering et al. 2011), which causes phosphorylation of Y338 on IL-2/IL-15R β , phosphorylating adaptor protein Shc, recruiting p-Shc to dock on Y338 (Friedmann, Migone et al. 1996), and in turn, activates Ras-dependent, MAPK-the extracellular signal-related kinase 1/2 (ERK1/2), PI3K/Akt, JAK/STAT, p38 α MAPK, Src family kinase signaling pathways. These signaling pathways will further induces the expression and activation of downstream NF- κ B signaling pathway (Mishra, Sullivan et al. 2014). Activation of these signaling pathways promotes Bcl-2 transcription and translation (Lai, Hou et al. 2013), Mcl-1 stabilization (Shenoy, Kirschnek et al. 2014), Bim degradation (Lai, Hou et al. 2013, Shenoy, Kirschnek et al. 2014) and production of cytokine and chemokine leading to increase cell proliferation, survival and immune activation.

Part IV. NF- κ B signaling pathway

Nuclear factor kappa B (NF- κ B) family transcription factors are important in the regulation of immune functions such as inflammation during injury and infection. (Napetschnig and Wu 2013). IL-15 has been reported to have the ability to activate NF-



κ B signaling pathways to promote cytokine (McDonald, Russo et al. 1998) and chemokine production (Chenoweth, Mian et al. 2012). The activation of NF- κ B signaling pathway needs activation of I κ B kinase (IKK) to phosphorylate I κ B which is the inhibitor of NF- κ B and lead to ubiquitination of I κ B by ubiquitin ligase following with its degradation by the 26S proteasome and release of NF- κ B for translocation to nucleus to activate gene transcription (Mathes, O'Dea et al. 2008). In addition, Although I κ B is mainly phosphorylated by IKK, p38 and AKT also may play a role in IL-15 triggered activation of NF- κ B. (Stone, Kastin et al. 2011) Therefore, IL-15 regulates NF- κ B activation in many aspects. Released NF- κ B can be phosphorylated by many kinases to enhance transactivation potential (Viatour, Merville et al. 2005).

Part V. Hypothesis of IL-15 Δ E7 structure

IL-15 Δ E7 has a partial deletion of the first 16 amino acids of exon 7 located in the helix B and partial loop A-B of IL15 protein (Tan and Lefrancois 2006). Analysis of the crystal structure of IL-15-IL-15R quaternary complexes has shown that the lacking of helix B and partial loop A-B in IL-15 Δ E7 might lose the binding of IL-15 Δ E7 to IL-15R α and γ c. Since the deletion is far from helices A and C the binding of IL-15 Δ E7 to IL-2/IL-15R β may not be changed.

Part VI. *Pichia* expression system

In order to produce IL-15 Δ E7 in higher quality and quantity, we applied the *Pichia* expression system. *Pichia pastoris* is a methylotrophic yeast which expresses alcohol oxidase (AOX) to metabolize methanol as its sole carbon source. The promoter which regulates the production of AOX is the one used to drive heterologous protein expression in *Pichia*. As a eukaryote, there are many advantages of using *Pichia pastoris* to produce recombinant protein such as posttranslational modification. Additionally, it is easier, faster and less expensive to generate protein of interest compared to other eukaryote expression systems. These features make *Pichia pastoris* useful for a powerful protein expression system. (Romanos, Scorer et al. 1992, Cregg and Higgins 1995)



Chapter II. Aims of the Study

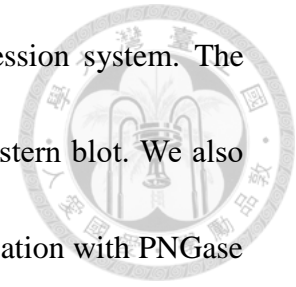


In our previous studies, we have demonstrated that an alternatively spliced IL-15 mRNA isoform which has partial deletion in exon 7 of IL-15 gene, namely IL-15 Δ E7 exerted differential function from prototype IL-15. Forced expression of IL-15 Δ E7 in normal mouse skin suppressed neutrophil infiltration to the inflamed skin induced by abrasion, sodium dodecyl sulfate or imiquimod treatment (Lee et al., 2015). Furthermore, *E.coli* IL-15 Δ E7/GST did not induce STAT5 phosphorylation, upregulation of *bcl-2* transcription and failed to support cytokine-dependent cell line, HT-2 cell proliferation and survival (Lee, Chang et al. 2015). These results provide evidence suggesting the immuno-regulatory role of IL-15 Δ E7 *in vivo* and *in vitro*. Nevertheless, how IL-15 Δ E7 exerts functions and regulates IL-15 mediated signaling remains unknown. In my thesis, experiments were designed to characterize the effects of IL-15 Δ E7 on cell survival, signaling activation and IL-15R α binding. These experiments were carried out by aims as follows.

1. Establishment of Yeast protein expression system to generate recombinant IL-15 Δ E7 and IL-15 protein

Although *E.coli* IL-15/GST induced STAT5 phosphorylation, it poorly supported overnight HT-2 cell culture. To generate high quantity and quality recombinant IL-15

and IL-15 Δ E7 for further research, we utilized the *Pichia* expression system. The secreted recombinant IL-15 and IL-15 Δ E7 were confirmed by Western blot. We also characterize protein properties using FPLC analysis and deglycosylation with PNGase



F. Bioactivity was measured with HT-2 cells by the MTT assay.

2. Functions of IL-15 Δ E7 on cell proliferation and survival

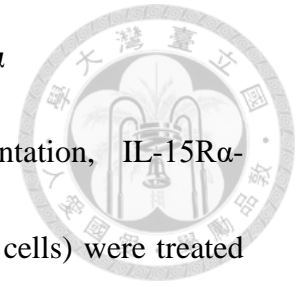
The HT-2 cells incubated with IL-15 or IL-15 Δ E7 were harvested at different time points. Treated HT-2 cells were stained with Annexin V and Propidium Iodide to measure percentages of viable cells or incubated with MTT for 4-6 h to estimate the number of live cells. The increased cell number of cytokine-treated HT-2 cells was measured by MTT assays.

3. Signalosome analysis of IL-15 Δ E7 induced signaling activation in HT-2 cells

To characterize IL-15 Δ E7 mediated signaling, untreated, IL-15 or IL-15 Δ E7 treated HT-2 cells were harvested at different time, and the lysates were analyzed with Micro-Western blotting to determine activation of signaling molecules. The results were then confirmed with conventional Western blotting.

4. Effects of IL-15 Δ E7 on the cell surface expression of IL-15R α

To investigate whether IL-15 Δ E7 regulates *trans*-presentation, IL-15R α -transduced and stably expressed in COS-7 cells (IL-15R α -COS-7 cells) were treated with IL-15 or IL-15 Δ E7. Treated cells were stained with anti-IL-15 antibody and analyzed by flow cytometry to compare binding affinity of IL-15 and IL-15 Δ E7 to IL-15R α . Furthermore, cells were also stained with anti-IL-15R α antibody followed by flow cytometry analysis to investigate downregulation of IL-15R α .



Chapter III. Materials and Methods



Part I. Methods

1. Cell lines and cell culture

The simian kidney epithelial cell line, COS-7, obtained from Dr. John Kung, (IMB Academia Sinica) was cultured in DMEM, supplemented with 10% FBS, 1 mM sodium pyruvate, and 20 mM HEPES. The cytokine-dependent murine T helper cell line, HT-2, kindly provided by Dr. Philippa Marrack (Denver, Colorado, USA), was cultured in MEM supplemented with 10% FBS and 10% tumor cocktail.

2. Construction of the X-33 strain expressing mouse IL-15 and IL-15 Δ E7

2.1 Construction of pPICZ α A-mIL-15(FLAG) and pPICZ α A-mIL-15 Δ E7(FLAG)

a. Preparation of mIL-15(FLAG) and mIL-15 Δ E7(FLAG)

Insert fragments of mIL-15(FLAG) and mIL-15 Δ E7(FLAG) were amplified by PCR from the templates pEF-mIL-15(FLAG) from Dr. Marrack Laboratory and pEF-mIL-15 Δ E7(FLAG) constructed in our laboratory, respectively. Furthermore, *Eco*RI and *Xba*I restriction enzyme sites were introduced to the 5' and 3' ends of these two insert fragments. The sequences of cloning primer set were described in the material



part. The PCR program was set as following:

1. 95°C denaturation interval for 5 min for 1 cycle
2. 95°C denaturation interval for 15 sec, followed by 63°C annealing interval for 15 sec, followed by 72°C elongation interval for 45 sec for 40 cycles
3. 72°C elongation for 7 min for 1 cycle.
4. Hold at 4°C.

The PCR products were then resolved on 0.8% agarose gel at 120 V for 30 min, followed by purification from agarose gel with the gel extraction kit. Purified PCR products were then digested with *Eco*RI (TaKaRa, 1040A) and *Xba*I (TaKaRa, 1093A) at 37°C for 1 hour, followed by DNA electrophoresis and gel purification with the gel extraction kit.

b. Preparation of pPICZ α A

The vector of pPICZ α A stored in TOP10 cells was kindly provided by Dr. Chien-Kuo Lee. The TOP10 cells with pPICZ α A were inoculated into 500 mL of low-salt LB medium with 25 ug/mL of zeocin (Invitrogen, R25005) and cultured at 37°C with shaking at 170 rpm overnight. The next day, TOP10 cells were centrifuged at 6000 rpm for 15 minutes and the supernatant was discarded. pPICZ α A was extracted from the pellet with the MIDI prep kit (QIAGEN, 12143). The extracted pPICZ α A was then digested with *Eco*RI and *Xba*I at 37°C for 1 hour. The digested pPICZ α A was then

purified through DNA electrophoresis and gel purification with the gel extraction kit.

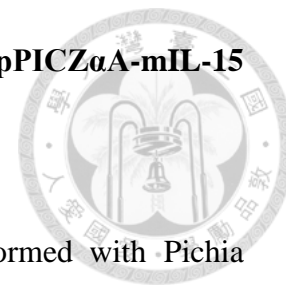
c. Ligation of mIL-15(FLAG) and mIL-15ΔE7(FLAG) to pPICZαA

The 10μL ligation reaction contained digested pPICZαA and digested mIL-15(FLAG) or digested mIL-15ΔE7(FLAG) in the molar ratio equal to 1:3. Total DNA amount of one reaction was 100 ng. 10x ligation buffer, T4 DNA ligase (Promega, M180A) and ddH₂O were included for ligation of pPICZαA to mIL-15(FLAG) or mIL-15ΔE7(FLAG). The ligation reaction was performed at 16°C overnight.

d. Transformation of pPICZαA-mIL-15ΔE7(FLAG) and pPICZαA-mIL-15(FLAG) into TOP10 cells

TOP10 cells were incubated with the product of ligation of pPICZαA-mIL-15ΔE7(FLAG) or pPICZαA-mIL-15 (FLAG) on ice for 30 minutes, followed by heating at 42°C for 90 seconds and then cooled on ice for 10 minutes. TOP10 cells were then cultured in 1 mL of SOC medium with shaking at 170 rpm for 2 hours at 37°C. Cultured TOP10 cells were spread on the LB agar plate containing 25 μg/mL of zeocin. The plate was placed in the 37°C incubator overnight for TOP10 cell growth. The next day colonies grown on the plates were selected and cultured in 3 mL of LB medium, followed by plasmid purification with the MINI prep kit. Purified plasmid was verified by digestion with *Eco*RI and *Xba*I or colony PCR, and the sequences was confirmed by DNA sequencing.

2.2 Transformation of pPICZ α A-mIL-15 Δ E7(FLAG) and pPICZ α A-mIL-15(FLAG) into the X-33 strain



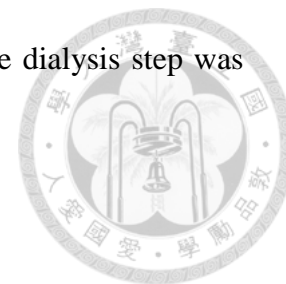
Competent cells preparation and transformation were performed with *Pichia* EasyComp™ Kit (Invitrogen, 45-0373). Colonies grown on the YPD plate containing 100 μ g/mL of zeocin were selected for genotyping with the *AOX1* primer set to verify if the mutation occurred.

3. Expression and purification of yeast recombinant IL-15 or IL-15 Δ E7

3.1 Induction of yeast recombinant IL-15 or IL-15 Δ E7

Transformed colony from the zeocin-selective plate was inoculated into 4 mL of BMGY and cultured at 30°C with shaking at 250 rpm overnight. Yeast in 4 mL was transferred to 500 mL of BMGY and grown at 30°C with shaking at 250 rpm for 1 day. The next day, yeast was centrifuged at 3000 rpm for 5 minutes, and the procedure of yeast amplification in 500 mL of BMGY was repeated for further amplification. Amplified yeast was pelleted and resuspended in 200 mL of BMMY. Resuspended Yeast was then grown at 20°C with shaking at 250 rpm for 4 days to induce extracellular recombinant IL-15 or IL-15 Δ E7 secretion. The methanol-induced yeast was centrifuged at 10000 rpm for 30 minutes. Supernatants were collected and filtered by 0.45 μ m filter cup, followed by dialysis against 5 L of pH8.0 TBS with 10 kDa MWCO

semi-permeable membrane (Thermo, 68100) at 4°C for 1 day. The dialysis step was repeated again.



3.2 Purification of yeast recombinant IL-15 or IL-15ΔE7

The supernatants from methanol-induced yeast were loaded to 5 mL of Ni-NTA column (GE healthcare, 17-5318-01) which was pre-equilibrated using equilibrium buffer. Then the column was washed with 50 mL of wash buffer to remove unbound proteins. The yeast recombinant IL-15 or IL-15ΔE7 was eluted with 15 mL of elution buffer. Eluted protein was then dialyzed against 1 L of pH equilibrium buffer with 10 kDa MWCO semi-permeable membrane at 4°C for 1 day. The dialysis step was repeated twice. Dialyzed protein was further filtered by 0.45 μm filter.

4. Deglycosylation analysis of yeast recombinant IL-15 and IL-15ΔE7

For deglycosylation analysis with PNGase F (New England Biolabs, P0704S) treatment, procedures were performed following the manufacturer's instructions. Briefly, yeast recombinant IL-15 or IL-15ΔE7 was mixed with water and 10X Glycoprotein denaturing buffer (New England Biolabs) and heated at 100°C for 10 minutes. Digestion with PNGase F was carried out in 1X GlycoBuffer 2 (New England Biolabs) and 1% NP-40 (New England Biolabs) at 37°C for 1 hour. The products were analyzed by Western blot.

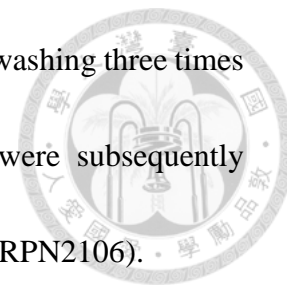
5. Coomassie blue staining of yeast recombinant IL-15 and IL-15ΔE7

For detection of IL-15 and IL-15ΔE7 on the 15% acrylamide gel, the gel was soaked in 25 mL of Coomassie blue staining solution at 4°C overnight. The next day, stained gel was destained in 25 mL of methanol destaining solution for at least 4 h. Replenish the methanol destaining solution several times until the background is fully destained.

6. Western blotting

For immunodetection of signaling molecules and IL-15 isoforms, cell lysates or recombinant protein samples were mixed in 6X denature sample buffer and heated on 95°C dry bath incubator for 10 minutes. For native condition, protein samples were mixed with 6X native sample buffer without 2-mercaptoethanol and were not heated at 95°C. The protein samples and prestained protein marker were resolved by 8~15% SDS-PAGE depending on protein molecular weight. Following separation, proteins were transferred to immune-P^{SQ} Membrane (Millipore) by a transfer unit (Transfer-Blot SD Semi-Dry Transfer Cell, Bio Rad). The membrane was blocked in 1% BSA in TBS-T (0.1% Tween 20 in TBS) for 1 hour at room temperature, and then probed with primary antibodies in 1% BSA in TBS-T at 4°C overnight. After washing three times for 10 min in TBS-T, the membrane was incubated with HRP-conjugated secondary

antibodies in 1% BSA for 1 hour at room temperature, followed by washing three times for 10 minutes in TBS-T. The immunoreactive protein bands were subsequently visualized by an enhanced chemiluminescence kit (GE Healthcare, RPN2106).



7. IL-15 and IL-15 Δ E7 biological assay using HT-2 cells

To evaluate the function of recombinant IL-15 and IL-15 Δ E7, HT-2 bioassay was performed and the viability of HT-2 cells was examined using MTT assay. HT-2 cells were washed in distilled PBS for three times. Recombinant IL-15 or IL-15 Δ E7 of required concentrations in 80 μ L of 10% CTM were added into the 96-well microtiter plate, followed by addition of 1×10^5 or 2×10^5 HT-2 cells/mL. By the second day of culture, 1/10 volume of 5 mg/mL MTT (3-(dimethylthiazol-2-yl)-2,5-diphenyl tetrazolium bromide; Sigma, M2128) in PBS was added into each well and the plate was incubated at 37°C for 4 to 6 hours. The MTT-derived crystals were subsequently dissolved in a mixture of 70% isopropanol, 30% water and 0.02 N HCl at 4°C overnight, and amount of conversion of MTT into a water insoluble purple compound by mitochondrial activity was determined by a microplate reader at OD595.

8. Flow cytometry analysis

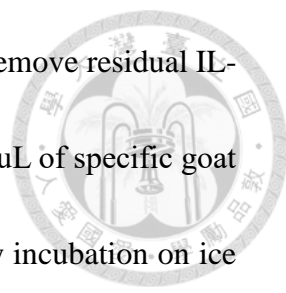


8.1 Apoptosis assay

HT-2 cells maintained in 10% CTM were centrifuged at 1000 rpm for 5 minutes, followed by aspiration of supernatants. Cells were then washed with 40mL of dPBS for three times. Washed HT-2 cells were resuspended in 10% CTM to the cell density of 2×10^5 cells/ml, and then treated with 150 ng/mL of IL-15, IL-15 Δ E7 or rIL-15 in a 24-well microtiter plate (1 mL/well). At indicated time, cells were resuspended and centrifuged at 1000 rpm for 5 minutes. Supernatants were aspirated and cell pellets were washed with 1mL of dPBS twice. Washed cells were resuspended in 100 μ L of $1 \times$ Annexin V binding buffer, followed by staining with 5 μ L of Annexin V-APC (BioLegend, 640932) and 2 μ L of Propidium Iodide (BioLegend, 640932) for 15 minutes in the dark. 400 μ L of $1 \times$ Annexin V binding buffer were then added to each staining. The stained cells were analyzed by a FACSCanto flow cytometer (BD Biosciences) and FlowJo software.

8.2 Immunodetection of expression of surface IL-15R α and surface attached IL-15 isoforms on IL-15R α -COS-7 cells

To detect surface IL-15R α and attached IL-15 isoforms expression on IL-15R α -COS-7 cells constructed in our lab, the cells were stained with anti-IL-15R α or anti-IL-



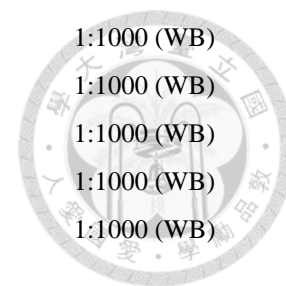
15 antibody. After being washed with cold staining buffer twice to remove residual IL-15 or IL-15ΔE7 in culture medium, the cells were stained with 100 uL of specific goat anti-mouse primary antibody diluted in staining buffer, followed by incubation on ice for 10 minutes. The cells were then washed twice with staining buffer and resuspended in 100 uL of rabbit anti-goat biotinylated secondary antibody diluted in staining buffer. After incubation on ice for 10 minutes and washed three times, cells were stained with streptavidin conjugated APC diluted in staining buffer for 5 minutes on ice. Cells were then washed with staining buffer twice and resuspended in 200 uL of staining buffer containing 1 uL of propidium iodide (BioLegend, 640932). The stained cells were analyzed by a FACSCanto flow cytometer (BD Biosciences) and FlowJo software.

Part II. Materials

1. List of antibodies

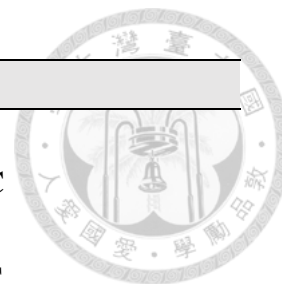
Antibodies	Supplier	Cat. No.	Dilution
Phospho-STAT5A/B(Tyr694/699)	Millipore	04-886	1:2000 (WB)
Phospho-p44/42 MAPK (Erk1/2)(Thr202/Tyr204)	Cell signaling	4370S	1:2000 (WB)
Phospho-Bim EL (Ser65)	Millipore	36-004	1:1000 (WB)
phospho-Myc(-c) (Thr58/Ser62)	Millipore	04-217	1:1000 (WB)
Bad (N-term)	Millipore	04-432	1:5000 (WB)
bcl-2	BD Transduction Laboratories™	610539	1:2000 (WB)
Bax antibody	Cell signaling	2772	1:1000 (WB)
Mcl-1	Millipore	MAB4602	1:200 (WB)

Phospho-Shc (Tyr317) Antibody	Cell signaling	2431S	1:1000 (WB)
Phospho-Src (Tyr527) Antibody	Cell signaling	2105S	1:1000 (WB)
phospho-Src (Tyr416), clone 9A6	Millipore	05-677	1:1000 (WB)
Phospho-Jak1 (Tyr1022/1023) Antibody	Cell signaling	3331	1:1000 (WB)
Phospho-Syk (Tyr525/526) (C87C1) Rabbit mAb	Cell signaling	2710S	1:1000 (WB)
Phospho-Jun(-c) (Ser63) (54B3) Rabbit mAb	Cell signaling	2361	1:1000 (WB)
Phospho-SAPK/JNK (Thr183/Tyr185) (81E11) Rabbit mAb	Cell signaling	4668S	1:1000 (WB)
Phospho-p38 MAPK (Thr180/Tyr182) (D3F9) XP™ Rabbit mAb	Cell signaling	4511S	1:1000 (WB)
IkappaB-alpha RabMAb®	Abcam	2466-1	1:500 (WB)
Phospho-SHP-2 (pY542) RabMAb®	Abcam	2184-1	1:1000 (WB)
phospho-GSK3 (Tyr279/Tyr216), clone 5G-2F	Millipore	05-413	1:500 (WB)
Phospho-IKKα/β (Ser176/180) (16A6) Rabbit mAb	Cell signaling	2697	1:1000 (WB)
IKKα/β Antibody (H-470)	Santa Cruz	sc-7607	1:1000 (WB)
Phospho-NF-kappa-B p65 (pS529) RabMAb®	Abcam	2884-1	1:1000 (WB)
Phospho-IkappaB-alpha (pS36) RabMAb®	Abcam	5740-1	1:1000 (WB)
NF-κB p65 Antibody (C-20)	Santa Cruz	sc-372-G	1:500 (WB)
Rabbit monoclonal antibody against Alpha-Tubulin	ORIGENE	TA307175	1:10000 (WB)
Goat anti-mouse-IL-15	R & D Systems	AF447	1:500 (WB) /1:200 (Flow)
Goat anti-mouse-IL-15Rα	R & D Systems	AF551	1:500 (WB) /1:200 (Flow)
ECL Rabbit IgG, HRP-linked whole Ab from donkey	GE Healthcare Life Sciences	NA934V	1:10000 (WB)
Donkey anti goat IgG	ImmunoJackson	705-006-147	1:10000 (WB)
ECL Mouse IgG, HRP-Linked Whole Ab (from sheep)	GE Healthcare Life Sciences	NA931V	1:10000 (WB)
Polyclonal Rabbit Anti-Goat Immunoglobulins/Biotinylated	Dako	E0466	1:200 (Flow)
Streptavidin-APC	Biolegend	405207	1:400 (Flow)



2. List of primers

Genes	Sequences (5'→3')
<i>AOX1</i> sequencing primer set	Forward primer: GACTGGTTCCAATTGACAAGC
	Reverse primer: GCAAATGGCATTCTGACATCC
Cloning primer set	Forward primer: CAGCGAATTCGCCAACTGGATAGATGTAAG
	Reverse primer: ATCCTCTAGACACTTGTCATCGTCGTCCTTGT



3. Solutions

3.1

10× D (20% Dextrose) in 1 liter

Dextrose	200 g
ddH ₂ O	1000 mL

Filter sterile and store at 4°C.

3.2

Yeast Extract Peptone Dextrose Medium (YPD) in 1 liter

Yeast Extract	10 g
Peptone	20 g
10× D	100 mL
ddH ₂ O	900 mL

1. Dissolve Yeast Extract and Peptone in 900 mL of ddH₂O followed by autoclaving for 20 min on liquid cycle.

2. Cool solution to ~60°C and add 100 mL of 10× D.

Add 1.0 mL of 100 mg/mL zeocin, if desired.

Include 20 g of agar if making YPD plates.

Store at 4°C.

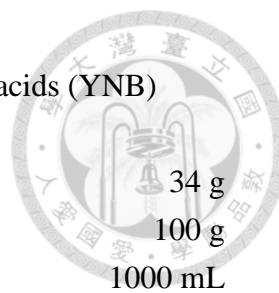
3.3

1M Potassium phosphate buffer, pH6.0 in 1 liter

1M K ₂ HPO ₄	132 mL
1M KH ₂ PO ₄	868 mL

Adjust the pH value to 6.0 and Sterilize by autoclaving.

Store at 4°C.



3.4

10× Yeast Nitrogen Base with Ammonium Sulfate without amino acids (YNB)
in 1 liter

YNB without Ammonium Sulfate and amino acids

Ammonium Sulfate

ddH₂O

34 g

100 g

1000 mL

Filter sterile after dissolving all compounds.

Store at 4°C.

3.5

500× B (0.02% Biotin) in 100 mL

Biotin

20 mg

ddH₂O

100 mL

Filter sterile after dissolving biotin.

Store at 4°C.

3.6

10× M (10% Methanol) in 100 mL

Methanol

10 mL

ddH₂O

90 mL

Filter sterile after mixing.

Store at 4°C.

3.7

10× GY (10% Glycerol) in 1 liter

Glycerol

100 mL

ddH₂O

900 mL

Sterilize by autoclaving.

Store at 4°C.

3.8

Buffered Glycerol-complex Medium (BMGY) in 1 liter

Yeast Extract

10 g

Peptone

20 g

1M Potassium phosphate buffer, pH6.0

100 mL

10× YNB

100 mL

500× B

2 mL

10× GY

100 mL

ddH₂O

700 mL

1. Dissolve Yeast Extract and Peptone in 700 mL of ddH₂O followed by autoclaving for 20 min on liquid cycle.
 2. Cool to room temperature and then add other solutions.
- Store media at 4°C.



3.9

Buffered Methanol-complex Medium (BMMY) in 1 liter

Yeast Extract	10 g
Peptone	20 g
1M Potassium phosphate buffer, pH6.0	100 mL
10× YNB	100 mL
500× B	2 mL
10× M	100 mL
ddH ₂ O	700 mL

1. Dissolve Yeast Extract and Peptone in 700 mL of ddH₂O followed by autoclaving for 20 min on liquid cycle.
 2. Cool to room temperature and then add other solutions.
- Store media at 4°C.

3.10

Equilibration Buffer (TBS) in 1 liter

Tris	6 g
NaCl	17.6 g
ddH ₂ O	900 mL

- Adjust the pH value to 8.0 and add ddH₂O to total volume of 1 L.
Store at 4°C.

3.11

Wash Buffer in 1 liter

Tris	6 g
NaCl	17.6 g
Imidazole	1.4 g
ddH ₂ O	900 mL

- Adjust the pH value to 8.0 and add ddH₂O to total volume of 1 L.
Store at 4°C.

3.12
Elution Buffer in 1 liter

Tris	6 g
NaCl	17.6 g
Imidazole	17 g
ddH ₂ O	900 mL

Adjust the pH value to 8.0 and add ddH₂O to total volume of 1 L.
Store at 4°C.

3.13
10× Phosphate buffered saline (PBS) in 1 liter

KCl	2 g
NaCl	80 g
Na ₂ HPO ₄	14.4 g
KH ₂ PO ₄	2.4 g
ddH ₂ O	900 mL

Adjust the pH value to 7.2 - 7.4 and add ddH₂O to total volume of 1 L.

3.14

Tumor cocktail in 1 liter

MEM	630 mL
Dextrose	7.5 g
50× Essential amino acids	75 mL
100× Non-essential amino acids	140 mL
100× Sodium pyruvate	100 mL
Adjust pH to 7.0.	
Add:	
Sodium bicarbonate	8.5 g
Gentamycin	500 mg
Penicillin G	600 mg
Streptomycin sulfate	1 g
2-Mercaptoethanol	34 uL

Sterilize with 0.22 um filter. Store in 45 mL aliquots at -20°C.





3.15

6× denature sample buffer in 100 mL

Tris base	4.2 g
Glycerol	30 mL
SDS	10 g
Bromophenol blue	12 mg
2-Mercaptoethanol	6 mL
ddH ₂ O	70 mL

Adjust the pH value to 6.8.

Discard 2-Mercaptoethanol if making native sample buffer.

Aliquots and store at -20°C.

3.16

10× SDS-PAGE running buffer in 1 liter

Tris	30.29 g
Glycine	187.7 g
SDS	10 g
ddH ₂ O	900 mL

Adjust the pH value to 8.1 - 8.8 and bring to 1 L with ddH₂O.

3.17

10× transfer buffer in 800 mL

Tris	58.2 g
Glycine	29.3 g
ddH ₂ O	700 mL

Adjust the pH value to 9.0 – 9.4 and bring to 800 mL with ddH₂O.

For 1 L of 1× transfer buffer, add 80 mL of 10× transfer buffer, 200 mL of methanol, and bring up to 1 L with ddH₂O.

3.18

SDS-PAGE separation gel (15% in 12 mL)

40% acrylamide	4.5 mL
1.5 M Tris + 0.4% SDS pH 8.8	3 mL
APS	150 uL
TEMED	15 uL
ddH ₂ O	4.34 mL

3.19

SDS-PAGE separation gel (5% in 3 mL)

40% acrylamide

1.5 M Tris + 0.4% SDS pH 8.8

APS

TEMED

ddH₂O

0.375 mL

0.38 mL

20 uL

5 uL

2.27 mL



3.20

Staining buffer in 500 mL

1× PBS

483 mL

FBS

10 mL

10% NaN₃

5 mL

0.5 M EDTA

2 mL

Store at 4°C.

3.21

Comassie Blue staining solution in 100 mL

Coomassie Brilliant R-250

0.25 g

Methanol

45 mL

Acetic acid

10 mL

ddH₂O

45 mL

Store at RT.

3.22

Methanol destaining solution in 1 L

Methanol

454 mL

Acetic acid

75 mL

ddH₂O

471 mL

Store at RT.

Chapter IV. Results



1. Expression and purification of Yeast recombinant IL-15 Δ E7 and IL-15

1.1 Strategy of constructing yeast plasmid expressing IL-15 Δ E7 or IL-15

To generate large amount of recombinant IL-15 Δ E7, we established *Pichia* expression system. The IL-15 Δ E7 gene was amplified from a template plasmid pEF-mIL-15 Δ E7(FLAG) by PCR technique and cloned into pPICZ α A to generate pPICZ α A-mIL-15 Δ E7(FLAG) (Figure 1). The pPICZ α A-mIL-15 Δ E7(FLAG) was then transformed into yeast X-33 strain and the yeast colonies which had correct insertion of IL-15 Δ E7 gene into the yeast chromosome were screened and confirmed (Figure 2 and Figure 3) . Since expression of the IL-15 Δ E7 gene was driven by the promoter of Alcohol Oxidase 1 gene (*AOX1*), treatment of transformed yeast with methanol induced the production of IL-15 Δ E7 from pPICZ α A-mIL-15 Δ E7(FLAG). Extracellular secretion of IL-15 Δ E7 was achieved by the cleavage of α -factor flanked with IL-15 Δ E7 by Yeast prohormone processing enzyme (*KEX2* gene product) (Yang, Kuang et al. 2013). Furthermore, IL-15 Δ E7 was purified from the culture medium over a Ni-NTA column. Mouse IL-15 was cloned in pPICZ α PICpPICZ α A-mIL-15(FLAG)) and the yeast recombinant IL-15 was generated and purified by following the same

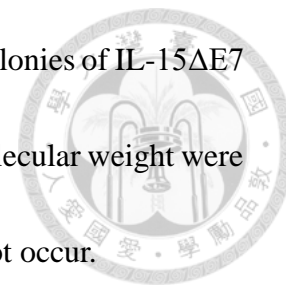
protocol as described above. Recombinant IL-15 and IL-15 Δ E7 proteins from yeast expression system was verified by Western blot analysis (Figure 4). The molecular weight of denatured IL-15 and IL-15 Δ E7 proteins were shown between 45-120 kDa for each protein on native gel (Figure 4A) and reduced to around 36 kDa on denature condition (Figure 4B). The size of yeast recombinant IL-15 or IL-15 Δ E7 protein was further reduced to about 17 kDa after treated with PNGase F to remove yeast cell-derived glycans (Figure 5).

1.2 Construction of recombinant IL-15 Δ E7 and IL-15 expressing X33 strain

Ligated pPICZ α IL-15 Δ E7(FLAG) and pPICZ α A-mIL-15(FLAG) was transformed into TOP10 cells followed by confirmation with restriction enzyme digestion or colony PCR (Figure 2). Eight colonies of IL-15 construct was selected and examined by *Eco*RI and *Xba*I digestion. We have found that six colonies were correct because mIL-15(FLAG) appeared on the gel at about 380 bps after restriction enzyme digestion (Figure 2A). On the other hand, the results of colony PCR of sixteen selected colonies of IL-15 Δ E7 construct have shown that one colony was correct (Figure 2B).

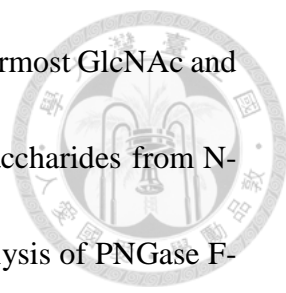
Verified IL-15 or IL-15 Δ E7 construct was transformed into the X-33 strain. Transformed yeast was selected on the zeocin selective YPD plate. Colonies grown on the YPD plate were analyzed with colony PCR. Four colonies of IL-15 construct were selected and verified, which shown that all were correct because of predicted bands at

about 900 bps appeared (Figure 3A). Similarly, 3 out of 6 selected colonies of IL-15ΔE7 construct were correct (Figure 3B). The PCR products at correct molecular weight were then purified and sent for sequencing to ensure that mutation did not occur.



1.3 Expression and characterization of yeast recombinant IL-15ΔE7 and IL-15

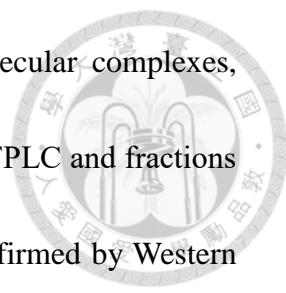
Transformed X-33 yeast strain were grown and amplified in Buffered Glycerol-complex Medium (BMGY) medium. When the yeast culture was at the log phase of growth, BMGY medium was replaced with Buffered Methanol-complex Medium (BMMY) to stimulate recombinant IL-15 or IL-15ΔE7 secretion. BMMY was collected when the amount of recombinant protein in medium did not increase. His-tagged yeast recombinant IL-15 or IL-15ΔE7 was then purified from collected BMMY over the Ni-NTA column. Purified IL-15 or IL-15ΔE7 was subjected to the native gel (Figure 4A) and denature gel (Figure 4B) for Western blot analysis. The expected size of recombinant IL-15 and IL-15ΔE7 protein was about 15-17 kDa. However, that of denatured IL-15 and IL-15ΔE7 proteins was shown between 45-120 kDa on native gel (Figure 4A) and reduced to around 37 kDa on denature condition (Figure 4B). Since recombinant human IL-15 is modified by N-linked glycosylation and the *P. pastoris* can add N-linked glycans on protein for secretion (Sun, Lai et al. 2016), the larger size of recombinant IL-15 and IL-15ΔE7 from yeast cells could result from N-linked glycosylation. Purified yeast recombinant IL-15 and IL-15ΔE7 proteins were denatured



and treated with PNGase F, an amidase that cleaves between the innermost GlcNAc and asparagine residues of high mannose, hybrid, and complex oligosaccharides from N-linked glycoproteins (Maley, Trimble et al. 1989). Western blot analysis of PNGase F-treated proteins showed that the molecular weight of yeast recombinant IL-15 and IL-15ΔE7 protein was reduced from about 30-35 kDa to 15-17 kDa (Figure 5). The size of *E.coli* derived recombinant mouse IL-15 was not affected by PNGase F treatment (Figure 5). These results revealed yeast recombinant IL-15 and IL-15ΔE7 were indeed N-glycosylated protein. Furthermore, the results also showed two bands in PNGase F-treated yeast recombinant IL-15 while only single band appeared in PNGase F treated yeast recombinant IL-15ΔE7 (Figure 5), suggesting that potential N-glycosylation sites existed in the first 16 amino acids of exon 7 which were deleted in IL-15ΔE7. In addition, other types of glycosylation such as O-glycosylation might occur in the spliced region in IL-15ΔE7 so that gave rise to different banding patterns between yeast recombinant IL-15 and IL-15ΔE7 after PNGase F treatment.

1.4 FPLC analysis of yeast recombinant IL-15ΔE7 and IL-15

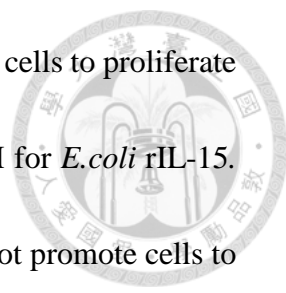
The higher molecular weight (over 100 kDa) of yeast recombinant IL-15 and IL-15ΔE7 run at native gel very likely resulted from the formation of multi-molecular protein complexes because the glycosylation modified by N-linked glycan would at most add 20 kDa on recombinant IL-15 and IL-15ΔE7 (Figure 4). To investigate



whether yeast recombinant IL-15 and IL-15ΔE7 form multi-molecular complexes, purified yeast recombinant IL-15 and IL-15ΔE7 were analyzed by FPLC and fractions containing IL-15 or IL-15ΔE7 were collected (Figure 6A) and confirmed by Western blot (Figure 6B). Fractions 8 through 13 of IL-15 and fractions 9 through 14 of IL-15ΔE7 were blotted by anti-IL-15 antibody, demonstrating all of these fractions were IL-15 and IL-15ΔE7, respectively. Since the molecular weight for each fraction ranged between over 500 kDa to 35 kDa, these results suggested that large protein complexes composed of different number of molecules be formed in IL-15 and IL-15ΔE7 (figure 6A). Treatment of HT-2 cells with yeast recombinant IL-15 from each fraction supported cell survival and proliferation (Figure 6C). These results confirmed that recombinant IL-15 and IL-15ΔE7 proteins produced from yeast expression system were modified by N-linked glycosylation. Despite the fact that multi-molecular protein complexes may form, they exerted bioactivity in the support of IL-15-dependent cell survival and proliferation.

1.5 Function analysis of yeast recombinant IL-15ΔE7 and IL-15

In the initial experiments, HT-2 cells were treated either with yeast recombinant IL-15 or with commercially purchased *E.coli*-derived IL-15 at various doses, and the numbers of viable cells were determined by MTT assay at 24 h. As is shown in Figure 7A (upper panels), yeast recombinant IL-15 supported HT-2 proliferation as was found

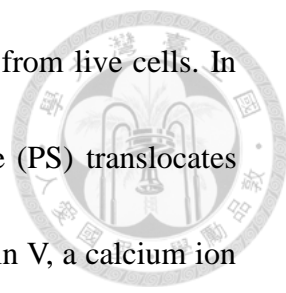


with *E.coli*-derived IL-15. The effective dose supporting 50% of the cells to proliferate (ED50) was 2 nM for yeast recombinant IL-15 and less than 70 pM for *E.coli* rIL-15. However, even the highest dose of yeast recombinant IL-15 could not promote cells to proliferate as well as the least dose of *E.coli* rIL-15 did. IL-15 Δ E7 did not support HT-2 cell survival at all doses (Figure 7A, lower panels). Although treatment of HT-2 cells with IL-15 immediately induced phosphorylation of STAT5 at 5 min and maintained up to 60 min after treatment, IL-15 Δ E7 failed to activate the phosphorylation of STAT5 (Figure 7B). The results were consistent with our previous experiments in which HT-2 cells were treated with recombinant GST-fusion IL-15 and GST-fusion IL-15 Δ E7 produced from *E.coli* (Lee, Chang et al. 2015). Since larger amount of functional recombinant IL-15 and IL-15 Δ E7 proteins can be made from yeast expression system, for the rest of the experiments in my thesis, yeast recombinant IL-15 and IL-15 Δ E7 were used unless they were specifically indicated otherwise.

2. Apoptosis and proliferation assay of IL-15 Δ E7 functions

2.1 Apoptosis assays of IL-15 Δ E7-treated HT-2 cells

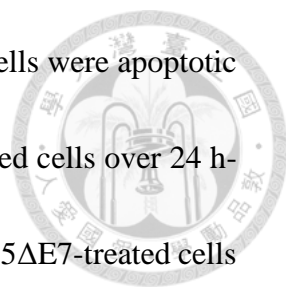
We have shown that IL-15 supported HT-2 cell proliferation while IL-15 Δ E7 failed to maintain HT-2 cell survival in the overnight culture. However, whether IL-15 Δ E7 promoted HT-2 cell apoptosis remained unclear. Therefore, we performed



Annexin V/Propidium Iodide assay to discriminate apoptotic cells from live cells. In the early stage of cell apoptosis, the membrane phosphatidylserine (PS) translocates from the inner side of the cell membrane to the cell surface. Annexin V, a calcium ion dependent phospholipid-binding protein, attaches to PS with high affinity. Therefore, fluorochrome-labeled Annexin V can be used to detect whether PS is exposed using flow cytometry. In the late stage of apoptosis, not only PS exposure occurs but also the integrity of the plasma membrane is disrupted. Consequently, propidium iodide (PI), a vital dye to stain nucleic acid, can penetrate into the nucleus of a cell which undergoes late apoptosis in which cell membrane integrity is lost. With simultaneous Annexin V and PI staining by flow cytometric analysis, cells that are Annexin V⁺ but PI⁻ are defined as early apoptotic cells; on the other hand, cells that are Annexin V and PI double positive cells are defined as late apoptotic cells. As is shown in Figure 8, HT-2 cells treated with camptothecin, the DNA topoisomerase inhibitor, underwent cell apoptosis (Figure 8A). Early apoptotic cells were observed at 6 h followed by the increase of late apoptotic cells up to 24 h (Figure 8B).

2.2 IL-15ΔE7 failed to support HT-2 cell survival.

In order to investigate the effects of IL-15ΔE7 on cell apoptosis, washed HT-2 cells were left untreated or treated with yeast recombinant IL-15 or IL-15ΔE7 followed by Annexin V/PI staining for flow cytometry analysis. Significant increase of apoptotic



cells was found in cytokine-deprived cells at 12 h and most of the cells were apoptotic at 24h (Figure 9A). Very little cell apoptosis occurred in IL-15 treated cells over 24 h-culture period. However, prominent cell apoptosis was found in IL-15 Δ E7-treated cells at 12 h and reached the same level as was found in untreated cells. HT-2 cells treated with commercially purchased rIL-15 showed a higher level of cell survival than our home-made yeast recombinant IL-15 (Figure 9A). The percentage of apoptotic cells in IL-15 Δ E7-treated cells ($20.9\% \pm 1.9\%$) was significantly higher than that in IL-15-treated cells ($1.8\% \pm 0.1\%$) at 12 h ($P < 0.005$). The difference became prominent at 24 h when the cells were treated with IL-15 Δ E7 ($99.2\% \pm 0.05\%$) compared with IL-15 treatment ($10.6\% \pm 0.3\%$) ($P < 0.001$) (Figure 9B). These results demonstrate that IL-15 Δ E7 does not promote cell death. Most of the cells died by apoptosis when they were cultured in IL-15 Δ E7-containing medium.

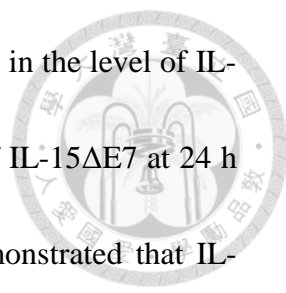
2.3 IL-15 Δ E7 failed to inhibit IL-15 mediated cell survival.

To investigate whether IL-15 Δ E7 blocked IL-15-mediated HT-2 cell survival, cytokine-deprived HT-2 cells were pre-treated with IL-15 Δ E7 for one hour followed by IL-15 treatment, or treated with the mixture of equal amount of IL-15 and IL-15 Δ E7. IL-15 alone treated HT-2 cells were also concluded as the non-IL-15 Δ E7 control. Cell apoptosis in each culture condition was assayed at 24 h by flow cytometry. The levels of Annexin⁺ cell apoptosis were comparable in HT-2 cells either subsequently treated

or simultaneously treated with IL-15ΔE7 compared with that in IL-15 alone treated cells (Figure 10A). The percentages of Annexin⁺ cells in each group showed no significant difference ($P = 0.24$) (Figure 10B). These results indicate that IL-15ΔE7 does not induce cell death in the presence of IL-15 nor block IL-15-mediated effect on cell survival.

2.4 IL-15ΔE7 fails to inhibit IL-15 mediated cell proliferation.

As is shown in Figure 11A, a dose-dependent cell proliferation was induced by IL-15 treatment by MTT assays. Significant cell proliferation was found in IL-15 treated cells at 150 ng/mL and peaked at 450 ng/ml at 24 h. More cells were proliferated at corresponding dose at 48 h. IL-15ΔE7 failed to induce HT-2 proliferation at all doses (Figure 11A). To further investigate whether IL-15ΔE7 had inhibitory effects on IL-15-mediated cell proliferation at a particular molar ratio, HT-2 cells were either treated with a mixture of fixed concentration of IL-15ΔE7 (150 ng/ml) and various amount of IL-15 (Figure 11B) or treated with a mixture of fixed concentration of IL-15 (150 ng/ml) with various amount of IL-15ΔE7 (Figure 11C). Treatment of 150 ng/mL of IL-15ΔE7 did not inhibit IL-15-mediated cell proliferation at any dose. The levels of cell proliferation in IL-15-treated cells were comparable with or without cotreatment of IL-15ΔE7 (Figure 11B). On the other hand, cells that were treated with 150 ng/mL of IL-15 proliferated at comparable levels among either treated with various amount of IL-

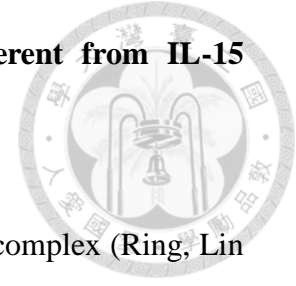


15ΔE7 or without cotreatment of IL-15ΔE7. No significant changes in the level of IL-15-mediated cell proliferation in the presence of various amount of IL-15ΔE7 at 24 h ($R^2=0.11$) and at 48 h ($R^2=0.22$) (Figure 11C). These results demonstrated that IL-15ΔE7 neither interfered with IL-15 induced cell survival nor inhibited IL-15 mediated cell proliferation.

3. Signalosome analysis of IL-15ΔE7 induced signaling activation in HT-2 cells

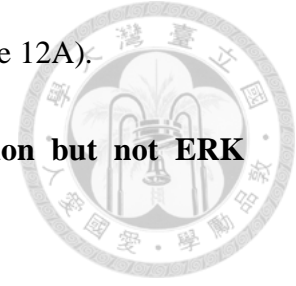
IL-15 activates JAK1/STAT3, PI3K/AKT, MAPK, Src family kinase and NF-κB pathways through IL-2/IL-15Rβ and JAK3/STAT5 through γ_c (Mishra, Sullivan et al. 2014, Jabri and Abadie 2015). Whether IL-15ΔE7 activates any of these signaling pathways and whether it has any effect on IL-15-mediated signaling remain to be clarified. Described experiments in the following section were performed by treating HT-2 cells with IL-15/GST, IL-15ΔE7/GST or GST alone. The cells were also treated with the mixture of equal amount of IL-15/GST and IL-15ΔE7/GST. The cell lysates were collected at indicated time and analyzed by Micro-Western analysis conducted at the Micro-Western Array core facility of National Health Research Institutes (NHRI) (Figure 12A).

3.1 IL-15 Δ E7 activated alternative signaling pathways different from IL-15 mediated responses.



Based on the structural analysis of quaternary IL-15 receptor complex (Ring, Lin et al. 2012), IL-15 Δ E7 may remain interaction with IL-2/IL-15R β . Therefore, we first focused on the analysis of IL-2/IL-15R β mediated downstream signaling in Micro-Western experiment. HT-2 cells maintained in IL-2 medium exerted lower levels of phosphorylation in IL-2R β -mediated signaling. After starvation, the phosphorylation level or quantity of all analyzed signaling molecules increased. IL-15/GST treatment induced more phosphorylation of p70 S6 kinase, PTEN, Shc, p38, JNK, jun, c-Myc, Src, Syk and SHP2 but not GSK3 (Figure 12A). IL-15 Δ E7/GST treatment also resulted in the increased levels of phosphorylation of p70 S6 kinase, pSrcY⁴¹⁶, pSrcY⁵²⁷, pSyk and pGSK3 compared with those in IL-15 treated cells (Figure 12B). Furthermore, IL-15 Δ E7/GST also triggered slightly higher levels of phosphorylation of JNK, c-Jun, p38 and c-Myc in MAPK pathways and PTEN in PI3K/AKT pathways. While IL-15/GST induced expression of bcl-2 but maintained unchanged expression of I κ B, IL-15 Δ E7/GST did not increase expression of bcl-2 but increase that of I κ B (Figure 12B). No significant differences occurred in the levels of pSHP2, pShc, bax and bad between IL-15 Δ E7/GST-treated and IL-15/GST treated cells (Figure 12A). HT-2 cells co-treated with IL-15/GST and IL-15 Δ E7/GST exerted similar patterns in the expression of these

signaling molecules as found in IL-15 Δ E7/GST treated cells (Figure 12A).

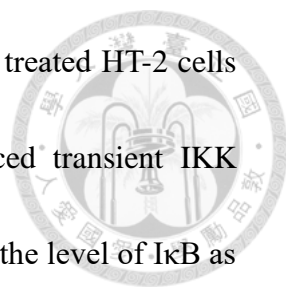


3.2 IL-15 Δ E7 induced JNK, P38 and SrcY⁴¹⁶ phosphorylation but not ERK phosphorylation.

MAPK molecules including pERK, pJNK and pP38 and pSrcY⁴¹⁶ were selected and analyzed by conventional immunoblotting method to confirm the results from Micro-Western experiments. HT-2 cells were left untreated or treated with yeast recombinant IL-15 or IL-15 Δ E7. As is shown in Figure 13, IL-15 induced the phosphorylation of ERK, JNK, P38 and SrcY⁴¹⁶. However, IL-15 Δ E7 failed to trigger ERK phosphorylation but enhanced the phosphorylation of JNK and SrcY⁴¹⁶. The level of phosphorylation of P38 was similar in HT-2 cells treated with IL-15 or IL-15 Δ E7 (Figure 13). In conclusion, IL-15 Δ E7 treatment activated JNK, P38 and SrcY⁴¹⁶ phosphorylation but not ERK phosphorylation as the results found in Micro-Western analysis.

3.3 IL-15 Δ E7 failed to induce phosphorylation of IKK but enhances phosphorylation of P65.

From the Micro-Western assay, we found that I κ B accumulated in IL-15 Δ E7 treated cells. It is well known that activation of NF- κ B pathways needs activation of IKK which induces I κ B degradation and release of NF- κ B from I κ B further phosphorylated by IKK (Lawrence 2009). We thus further analyzed phosphorylation of

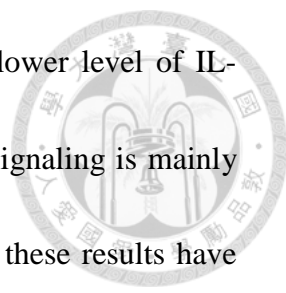


IKK, degradation of I κ B and phosphorylation of P65 in IL-15 Δ E7 treated HT-2 cells by Western blot analysis. We found that IL-15 treatment induced transient IKK phosphorylation, downstream P65 phosphorylation while remained the level of I κ B as shown in untreated cells. From the results of IL-15 treatment, NF- κ B was not activated in HT-2 cells due to unaltered I κ B levels although IKK was transiently activated. However, IL-15 Δ E7 treatment failed to induce IKK phosphorylation but enhanced phosphorylation of P65. The level of I κ B in HT-2 cells did not alter after IL-15 Δ E7 treatment. Similar to results of IL-15 treatment, NF- κ B was not activated in IL-15 Δ E7 treated HT-2 cells because the level of I κ B was not reduced. We concluded that NF- κ B was not activated in IL-15 and IL-15 Δ E7 treated HT-2 cells. HT-2 cells are not appropriate for research on NF- κ B pathways. Furthermore, more results are in need for investigation of the role of IL-15 Δ E7 in NF- κ B pathways such as translocation of NF- κ B into the nucleus.

4. Effects of IL-15 Δ E7 on the cell surface expression of IL-15R α

4.1 The reasons of investigating the role of IL-15 Δ E7 to *trans*-presentation

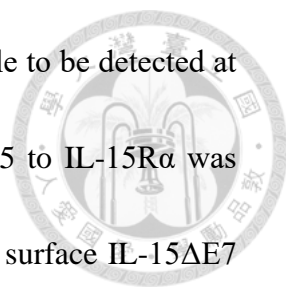
In my previous experiments, I have demonstrated that IL-15 Δ E7 did not activate γ c-mediated phosphorylation of STAT5 but partially activated IL-2/IL-15R β -mediated signaling in HT-2 cells. However, IL-15 Δ E7 did not block IL-15-mediated



phosphorylation of STAT5, cell proliferation and survival. Since lower level of IL-15R α than IL-2/IL-15R β and γ_c is expressed on HT-2 and IL-15 signaling is mainly dependent on IL-2/IL-15R β and γ_c (Mishra, Sullivan et al. 2014), these results have suggested that the *cis*-binding of IL-15 to IL-2/IL-15R β and γ_c receptor complex was not inhibited by IL-15 Δ E7. It is well accepted that IL-15 can be presented in *trans* to IL-2/IL-15R β and γ_c expressed on neighboring cells (Dubois, Mariner et al. 2002, Jabri and Abadie 2015). Whether IL-15 Δ E7 had a regulatory role in the *trans*-presentation by IL-15R α remains unknown. In the following section, I will describe the results obtained from experiments in which IL-15 Δ E7 was added to the IL-15R α overexpressing COS-7 cell line (IL-15R α -COS-7) and investigated the effects of IL-15 Δ E7 on the surface expression of IL-15R α by flow cytometry.

4.2 IL-15 Δ E7 bond to IL-15R α with an extremely low affinity.

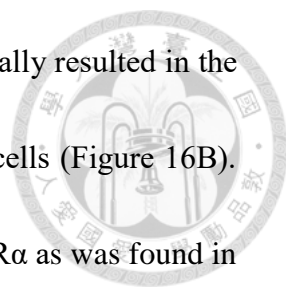
It is well known that IL-15 associates with IL-15R α with high affinity ($K_d = 10^{-11}$ M) (Ring, Lin et al. 2012) and is *trans*-presented by IL-15R α to IL-2/IL-15R β and γ_c expressing cells (Jabri and Abadie 2015). However, whether IL-15 Δ E7 binds to IL-15R α remains uncertain. To measure the affinity of IL-15 Δ E7 to IL-15R α , dislodged IL-15R α -COS-7 cells were left untreated or treated with various amount of yeast recombinant IL-15 or IL-15 Δ E7 for 2 h on ice to prevent receptor internalization (Zhao and French 2013). Cells were then stained with anti-IL-15 antibody and analyzed by



flow cytometry. We found that binding of IL-15 to IL-15R α was able to be detected at minimal concentration of 10^{-8} M and the level of binding of IL-15 to IL-15R α was increased in a dose-dependent manner (Figure 15A). Nevertheless, surface IL-15 Δ E7 was not detected in IL-15R α -COS-7 cells treated with IL-15 Δ E7 even at 10^{-8} M and no binding was found up to 10^{-6} M. (Figure 15A). Although expression of IL-15R α was downregulated on the surface of IL-15R α -COS-7 cells by IL-15 treatment at 10^{-6} M, the levels of surface expression of IL-15R α were comparable in IL-15-treated and IL-15 Δ E7-treated cells ranged between 10^{-7} M and 10^{-10} M (Figure 15B). These results showed that IL-15 Δ E7 poorly ligated to IL-15R α at a very low affinity for IL-15R α compared with IL-15.

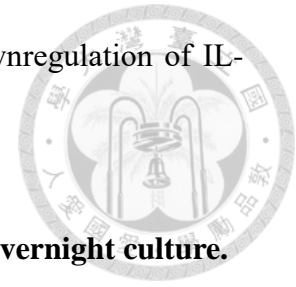
4.3 Time course analysis of surface IL-15R α downregulation induced by IL-15 Δ E7

It has been shown that binding of IL-15 to IL-15R α triggers the receptor internalization into the endosome followed by the recycle of IL-15R α back to the plasma membrane (Dubois, Mariner et al. 2002, Sato, Patel et al. 2007). To find out whether IL-15 Δ E7 triggered the changes in the surface expression of IL-15R α , dislodged IL-15R α -COS-7 cells were left untreated or treated yeast recombinant IL-15 or IL-15 Δ E7 at 37°C. At different time points, cells were harvested and stained with anti-IL-15R α antibody for flow cytometry analysis. We found that the surface expression of IL-15R α gradually decreased in untreated cells (Figure 16A). IL-15



treatment induced rapid downregulation of surface IL-15R α and finally resulted in the less level of IL-15R α expression compared with that of untreated cells (Figure 16B). IL-15 Δ E7 treatment did not reduce the surface expression of IL-15R α as was found in IL-15-treated cells (Figure 16C). We also calculated the percentage of reduction in surface IL-15R α in IL-15 or IL-15 Δ E7 treated cells compared with that of untreated cells at each time point (Figure 16D). We found that IL-15 treatment reduced the surface expression of IL-15R α by 28% in the initial 30 min, the reduction became 58% within 2 hours and remained stable up to 6 h after treatment (Figure 16E). However, surface expression of IL-15R α was stable in IL-15 Δ E7-treated IL-15R α -COS-7 cells over 4 h treatment and reduced by 45% at 6 h. We also measured the reduction rate of surface IL-15R α expression. The results showed that reduction rate of untreated cells within the first 0.5 hours was 1968 Δ MFI/ Δ hr, and then maintained at about 600 Δ MFI/ Δ hr between 0.5 hour and 6 hour. IL-15 treatment induced rapid reduction of surface IL-15R α expression at the rate of 5044 Δ MFI/ Δ hr within the first 0.5 hours. The reduction rate of surface IL-15R α expression in IL-15 treated cells gradually decreased afterwards. The reduction rate in IL-15 Δ E7 treated cells was similar with that of untreated cells in each time interval but slightly increased between 4 hour and 6 hour (untreated cells: 723 Δ MFI/ Δ hr, IL-15 Δ E7 treated cells: 1045 Δ MFI/ Δ hr). These results demonstrated that while IL-15 bond to IL-15R α and downregulated the surface expression of IL-15R α ,

IL-15ΔE7 poorly bond to IL-15Rα and resulted in a delayed downregulation of IL-15Rα from the cell surface.



4.4 IL-15ΔE7 induced surface IL-15Rα downregulation in the overnight culture.

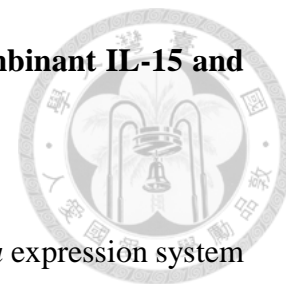
To investigate the long-term effects of IL-15 or IL-15ΔE7 on the surface expression of IL-15Rα, dislodged IL-15Rα-COS-7 cells were left untreated or treated with various amount of yeast recombinant IL-15 or IL-15ΔE7 overnight at 37°C, followed by staining with anti-IL-15Rα antibody for flow cytometry analysis. We found that downregulation of IL-15Rα expression by IL-15 was in a dose-dependent manner (Figure 17A). While the expression levels of IL-15Rα were comparable in IL-15-treated and IL-15ΔE7-treated cells at the concentration ranged from 10⁻⁸ M to 10⁻¹⁰ M, IL-15ΔE7 treatment failed to induce further reduction of IL-15Rα surface expression at the dose of 10⁻⁷ M as was found in cells treated with IL-15 at the same concentration (Figure 17B). These results demonstrated that IL-15 bond to IL-15Rα and induced decreased surface IL-15Rα expression in a dose-dependent manner. Nevertheless, IL-15ΔE7 was bond to IL-15Rα with very low affinity and triggered marginal downregulation of surface IL-15Rα expression at high dose (Figure 17C). The biological meaning of IL-15ΔE7 induced downregulation of IL-15Rα surface expression needs more investigation.

Chapter V. Discussion



IL-15 Δ E7 is generated from the alternatively spliced IL-15 mRNA and constitutively expressed in murine intestinal tissues (Tan and Lefrancois 2006). Our previous results found that IL-15 Δ E7 did not activate the phosphorylation of STAT5 and inhibited the transcription of *bcl-2* mRNA (Lee, Chang et al. 2015). To further characterize the functions of IL-15 Δ E7, in this thesis, I have successfully established *Pichia* yeast expression system to produce recombinant IL-15 Δ E7 and IL-15, individually. As with previous findings (Lee, Chang et al. 2015), yeast recombinant IL-15 Δ E7 failed to support IL-15 dependent cell proliferation and survival. IL-15 Δ E7 did not enhance cell death in treated cells but rather it failed to transduce optimal signalosome for cell activation. However, the cells proliferated well to IL-15 treatment when the cells were pretreated or co-treated with IL-15 Δ E7. Furthermore, IL-15 Δ E7 was shown to poorly bind to IL-15R α with very low affinity. IL-15 Δ E7 induced delayed downregulation of IL-15R α surface expression but caused comparable reduction of IL-15R α surface expression compared with IL-15 in the overnight culture.

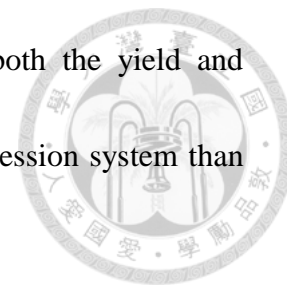
1. Establishment of *Pichia* expression system to generate recombinant IL-15 and IL-15ΔE7



To investigate the function of IL-15ΔE7, we established *Pichia* expression system to produce recombinant IL-15ΔE7 and IL-15 for parallel comparison. Yeasts are eukaryotes. Recombinant proteins generated in yeast expression system can undergo several post-translational modifications such as protein folding and glycosylation which are lacked in bacterial expression system. In other words, yeast recombinant proteins could possibly yield bioactivities that are more similar to *de novo* proteins expressed in the mammalian cells (Sun, Lai et al. 2016). Results from our experiments showed that the cell proliferation and survival of HT-2 cells were supported by *E.coli* IL-15/GST at much more than 1000 ng/ml compared with these by much less dose of yeast recombinant IL-15 protein (100 ng/ml) .

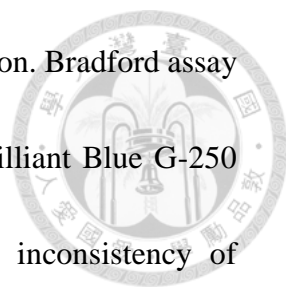
A recent publication describing an improved protocol for generating recombinant human IL-15 from *Pichia* yeast cells addressed the critical conditions to enhance production efficiency (Dragosits, Stadlmann et al. 2009, Zhong, Yang et al. 2014). Accordingly, when I double the volume of medium for yeast culture and replaced it with fresh medium at steady phase as well as to change the culture temperature from 30°C to 20°C, the yield of the protein in the culture supernatant was greatly increased by 4-8 fold. It reached up to 2.5 mg/L. Although time required to complete the

production process is longer than that from bacterial system, both the yield and solubility of the recombinant protein are enhanced by *Pichia* expression system than that by *E.coli* (0.6 mg/L).



FPLC analysis of yeast recombinant IL-15 and IL-15 Δ E7 showed that high number of multi-molecular protein complexes was formed when protein concentration was attempted to increase by condensation. Similar patterns for yeast recombinant IL-15 and IL-15 Δ E7 shown on native gel and denature gel by Western blotting suggested that both proteins were similarly produced from the yeast cells. In addition to the formation of multi-protein complexes in solution, high molecular weight forms observed in native IL-15 and IL-15 Δ E7 (Figure 4) were possibly due to N-glycosylation because the signal was reduced after treated with PNGase F (Figure 5).

Furthermore, I have also performed Coomassie blue staining of yeast recombinant IL-15 and IL-15 Δ E7 and *E.coli* recombinant IL-15 to confirm purity (Figure A.1.). However, even though yeast recombinant IL-15 and IL-15 Δ E7 were deglycosylated with PNGase F to decrease smears caused by polydisperse glycosylation, the banding intensity of 10 ug deglycosylated IL-15 and IL-15 Δ E7 was much lower than same amount of BSA. The stock concentration of yeast recombinant IL-15 and IL-15 Δ E7 was determined by OD280 measurement and Bradford assay. Because phenylalanine, tyrosine and tryptophan contains the aromatic ring contributing to absorbance at



wavelength of 280 nm, OD280 can represent the protein concentration. Bradford assay is to measure OD595 resulting from absorbance of Coomassie Brilliant Blue G-250 when binding to protein to acquire protein concentration. The inconsistency of measured protein concentration and banding intensity demonstrates that other non-IL-15 or non-IL-15 Δ E7 protein may exist in the yeast recombinant IL-15 and IL-15 Δ E7. Although there is one band in each lane of yeast recombinant IL-15 and IL-15 Δ E7, the purity may not be as good as we have thought.

2. The regulatory functions of IL-15 Δ E7 on HT-2 cells

In this study, I used the IL-2/IL-15 dependent helper T cell line (HT-2) to compare cytokine functions of IL-15 Δ E7 versus IL-15. Since the survival and proliferation of HT-2 cells are absolutely dependent on IL-2 or IL-15, alterations in transducing activation signaling by IL-15 Δ E7 can be easily observed. While HT-2 cells proliferated to IL-15 in the dose-dependent manner, IL-15 Δ E7-treated cells at corresponding doses as in IL-15 treated cells died in overnight culture (Figure 7A and 9). We demonstrated that IL-15 Δ E7 did not trigger an earlier onset of cell apoptosis compared with IL-15-treated cells. The loss of cell viability in IL-15 Δ E7-treated cells was very likely caused by the inhibition of IL-15 Δ E7-mediated signal transduction for cell survival. We also found that addition of IL-15 Δ E7 to IL-15 treated cells did not promote cell apoptosis

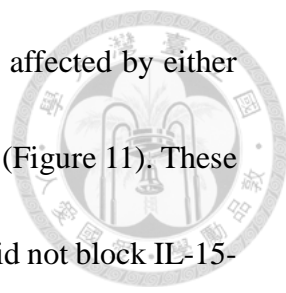
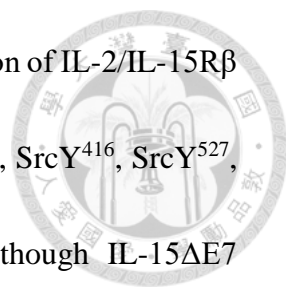


(Figure 10). IL-15 mediated cell survival and proliferation was not affected by either simultaneous or subsequent (one hour apart) treatment of IL-15 Δ E7 (Figure 11). These experiments demonstrated exogenous IL-15 Δ E7 even at high dose did not block IL-15-mediated cell proliferation. Since very low level of IL-15R α is expressed by HT-2 cells and the cytokine effects are mainly transduced through IL-2/IL-15R β / γ_c receptor complexes, results from these experiments have suggested that while IL-15 Δ E7 failed to support HT-2 cell survival and proliferation, it did not block the binding of IL-15 to IL-2/IL-15R β / γ_c receptor complexes.

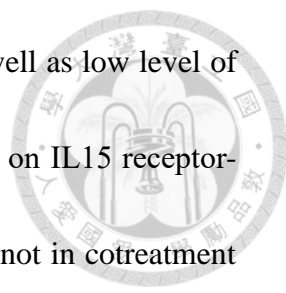
3. Analysis of IL-15 Δ E7 mediated signaling pathways

IL-15 induces signaling through IL-2/IL-15R β and γ_c receptor complexes. Our experiments demonstrated that IL-15 Δ E7 failed to support IL15-dependent cell proliferation, suggesting that IL-15 Δ E7 might either loss the binding to IL-2/IL-15R β and γ_c or transduce differential signal compared to IL-15. According to information from the structural analysis of quaternary IL-15 receptor complex (Ring, Lin et al. 2012), deletion of the first 16 amino acids of exon 7 in IL-15 Δ E7 is likely to have a greater impact on the interaction with γ_c rather than on that with β subunit (Ring, Lin et al. 2012). Indeed, IL-15 Δ E7 did not activate the phosphorylation of STAT5 in T cell line. Micro-Western analysis of IL-15R β mediated signalosomes in IL-15 Δ E7-treated



cells showed that IL-15 Δ E7 activated higher levels of phosphorylation of IL-2/IL-15R β mediated downstream signaling molecules including p70 S6 kinase, SrcY⁴¹⁶, SrcY⁵²⁷, Syk, GSK3 compared with IL-15-treated cells (Figure 12). Although IL-15 Δ E7 activated MAPK signaling including JNK, P38 and P65, phosphorylation of ERK and IKK α β were blocked in IL-15 Δ E7-treated cells (Figure 13 and 14). These experiments demonstrated that interaction of IL-15 Δ E7 with IL-2/IL-15R β and γ_c receptor complexes resulted in the block of STAT5 activation as well as inducing less optimal signaling to support cell survival and proliferation.

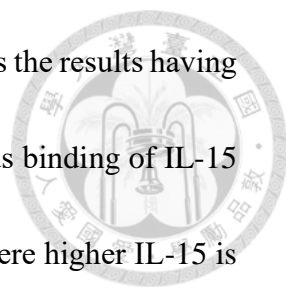
We also investigated IL-15 Δ E7 impacts on IL-15 mediated signaling. Signalosome analysis of co-treated HT-2 cells has shown that IL-15 Δ E7 was able to modify IL-15 mediated β chain signaling because downstream molecules from cotreatment were phosphorylated in the level similar to those of IL-15 Δ E7 treatment (Figure 12). IL-15 induced ERK phosphorylation were inhibited by IL-15 Δ E7 treatment while STAT5 phosphorylation was not affected. However, results of proliferation and apoptosis assays have told us that exogenous addition of IL-15 Δ E7 did not block IL-15 induced proliferation and survival. From structural analysis of quaternary IL-15 receptor complex, we suggest that IL-15 Δ E7 have low affinity for dimeric IL-2/IL-15R β / γ_c complex because reduced length of IL-15 Δ E7 resulted in poor binding to γ_c (Ring, Lin et al. 2012). Dimeric IL-2/IL-15R β / γ_c complex occupied IL-15 may not be replaced



with IL-15 Δ E7. Since HT-2 cells express IL-2/IL-15R β and γ_c as well as low level of the IL-15R α on the cell surface, the inhibitory effects of IL-15 Δ E7 on IL15 receptor-mediated signaling was only present when it was singly added but not in cotreatment condition. Our experiments demonstrated that IL-15 Δ E7 failed to suppress IL-15 function on T cells even at 27-fold higher concentration than IL-15. These results suggested that IL-15 Δ E7 may have limited role in interfering IL-15 when it was *cis*-presented to receptor complexes. In conclusion, IL-15 signaling through *cis*-presentation to IL-2/IL-15R β and γ_c is sufficient for HT-2 cell survival and proliferation regardless of IL-15 Δ E7 presentation.

4. The differences in affinity and regulation of surface IL-15R α between IL-15 and IL-15 Δ E7

One of the distinct mechanisms by which IL-15 transduces signal to target cells is through the trans-presentation by IL-15R α expressed on other cells (Dubois, Mariner et al. 2002, Jabri and Abadie 2015). Structural analysis of quaternary IL-15 receptor complex has shown that IL-15R α binds to A-B and C-D loops and in turn stabilizes four helices of IL-15, which increases affinity of IL-15 to dimeric IL-2/IL-15R β / γ_c complex by 150-fold (Ring, Lin et al. 2012). IL-15 Δ E7 lacks partial A-B loop and most of the helix B in which important IL-15/IL-15R α binding site, Glu-46, is located (Olsen,



Ota et al. 2007). We suggest that IL-15 Δ E7 poorly bind to IL-15R α as the results having shown that undetectable IL-15 Δ E7 ligated to IL-15R α while obvious binding of IL-15 to IL-15R α was observed (Figure 15A). In physiologic situation where higher IL-15 is produced than IL-15 Δ E7, IL-15 Δ E7 might not be directly presented to cells through *trans*-presentation.

IL-15 has been reported to induce internalization of the IL-15/IL-15R α complex after complex formation (Dubois, Mariner et al. 2002). The results have shown that IL-15 treatment induced rapid and dramatic downregulation of surface IL-15R α expression in IL-15R α -COS-7 cells in 2 hours (Figure 16B). However, IL-15 Δ E7 failed to induce IL-15R α internalization initially but caused obvious delayed decreased expression level of IL-15R α at 6 hour (Figure 16C). These results enlightened us to consider long-term effects of IL-15 Δ E7 on regulation of IL-15R α surface expression. Although IL-15 Δ E7 induced marginal decrease of surface IL-15R α expression at high dose compared with IL-15, about 30% downregulation of surface IL-15R α expression was induced in IL-15 Δ E7 treated cells (Figure 17C). It is known that *trans*-presentation of IL-15 by IL-15R α on myeloid cells is important for T cells and NK cells to develop effector functions such as virus clearance (Jabri and Abadie 2015). Downregulation of surface IL-15R α expression by IL-15 Δ E7 possibly results in reduced number of available IL-15R α for IL-15, which inhibits IL-15 responses. Indeed, we have observed decreased

number of memory T cells and downregulated inflammatory responses in P191 mice expressing IL-15 Δ E7 and IL-15 at comparative level (Lee, Chang et al. 2015). Therefore, the role for IL-15 Δ E7 in regulating IL-15 function via *trans*-presentation is worth of further investigation.

5. The connection between *in vitro* experiments and P191 mouse phenotypes

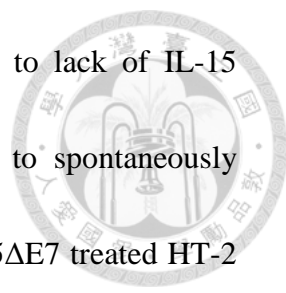
The P191 mouse which expresses same level of IL-15 and IL-15 Δ E7 mRNA has decreased number of memory T cells. Reduced keratinocyte activation and inhibition of neutrophil infiltration were also observed in P191 skin, P191 skin graft transplanted onto the WT host and WT skin expressing IL-15 Δ E7 ectopically in response to mechanical stimulation (Lee, Chang et al. 2015). These results demonstrate that IL-15 Δ E7 has regulatory functions on inflammation. In addition, unlike IL-15, IL-15 Δ E7 fails to activate STAT5 phosphorylation and *bcl-2* transcription important for HT-2 cell survival (Lee, Chang et al. 2015), suggesting IL-15 Δ E7 possibly regulates inflammation by enhancing immune cell apoptosis. However, the results of apoptosis and proliferation assay have shown that IL-15 Δ E7 failed to induce earlier HT-2 cell apoptosis and inhibit IL-15 promoted HT-2 cell survival and proliferation.

Different from P191 mouse models, only HT-2 cell was involved in the *in vitro* system, which demonstrated that IL-15 Δ E7 should not directly influence IL-15

responsive cells to perform regulatory functions. In *in vivo* conditions, IL-15 is usually presented by IL-15/IL-15R α expressing cells *in trans* to neighboring IL-2/IL-15R β / γ_c expressing cells. Direct exogenous addition of IL-15 and IL-15 Δ E7 to HT-2 cells may not be an adequate way to explore IL-15 Δ E7 functions.

We have discovered that IL-15 Δ E7 caused downregulated IL-15R α surface expression (Figure 16 and 17). These data implicate that IL-15 Δ E7 may regulate inflammation through reducing amount of IL-15/IL-15R α complexes on cell surface to inhibit IL-15 *trans*-presentation to IL-2/IL-15R β / γ_c expressing cells. Furthermore, it has been reported that IL-15 can signal through IL-15R α to activate NF- κ B as the transcription factor for chemokines and cytokines (Stone, Kastin et al. 2011, Chenoweth, Mian et al. 2012, Burke, Lu et al. 2014). Downregulation of abrasion induced KC/CXCL1 and G-CSF expression and neutrophil infiltration observed in WT skin ectopically expressing IL-15 Δ E7 may correlate with reduced surface IL-15R α expression caused by IL-15 Δ E7 because less NF- κ B can be activated (Lee, Chang et al. 2015).

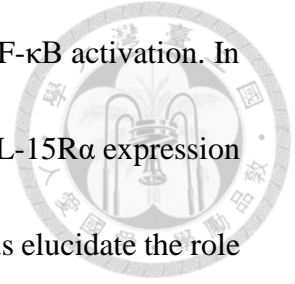
However, although IL-15^{-/-} mouse lacks memory CD8⁺ T cells (Boyman, Krieg et al. 2012), keratinocyte activation and neutrophil infiltration induced by abrasion are still observed in IL-15^{-/-} skin whose cells do not present IL-15/IL-15R α complexes on cell surface at all (Lee, Chang et al. 2015). These results implicate that inflammation



suppression by ectopic expression of IL-15 Δ E7 is not only due to lack of IL-15 presentation. IL-15 Δ E7 possibly transduces alternative signaling to spontaneously regulate inflammation. According to signalosome analysis of IL-15 Δ E7 treated HT-2 cells, IL-15 Δ E7 activated IL-2/IL-15R β mediated signaling but failed to induce phosphorylation of STAT5, ERK and IKK (Figure 13 and 14). In addition to promoting T cell and neutrophil survival and proliferation, STAT5 and ERK activation also induces downstream activation and expression of NF- κ B (Mishra, Sullivan et al. 2014, Jabri and Abadie 2015). Furthermore, IKK is responsible for I κ B degradation and NF- κ B phosphorylation and translocation into the nucleus. Inactivation of STAT5, ERK and IKK will result in inactivation of NF- κ B, which further causes inhibition of chemokines and cytokines expression. Although we are not certain if IL-15 Δ E7 inhibits STAT5, ERK and IKK activation spontaneously, it is possible that IL-15 Δ E7 regulates inflammation through blockade of NF- κ B activation to prevent chemokines and cytokines expression.

By comparing *in vitro* experiments and P191 mouse phenotypes, IL-15 Δ E7 is more likely to regulate surface IL-15R α expression and thereby control IL-15 *trans*-presentation and downregulate IL-15R α mediated NF- κ B activation rather than directly act on IL-15 responsive cells to induce cell apoptosis to suppress inflammation. Furthermore, IL-15 Δ E7 possibly spontaneously induces inhibitory signaling to regulate

chemokines and cytokines expression through downregulation of NF- κ B activation. In the future, further investigation of how IL-15 Δ E7 controls surface IL-15R α expression and IL-15 *trans*-presentation as well as NF- κ B activation will help us elucidate the role of IL-15 Δ E7 in regulation of inflammation.



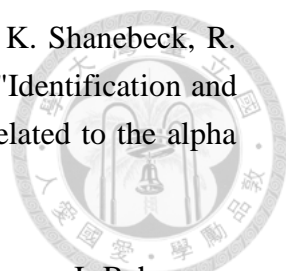
References

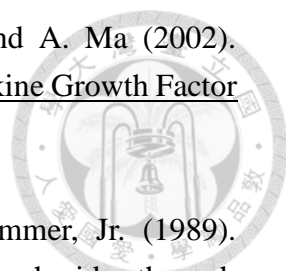


1. Ben Ahmed, M., N. Belhadj Hmida, N. Moes, S. Buyse, M. Abdeladhim, H. Louzir and N. Cerf-Bensussan (2009). "IL-15 renders conventional lymphocytes resistant to suppressive functions of regulatory T cells through activation of the phosphatidylinositol 3-kinase pathway." J Immunol **182**(11): 6763-6770.
2. Bergamaschi, C., R. Jalah, V. Kulkarni, M. Rosati, G. M. Zhang, C. Alicea, A. S. Zolotukhin, B. K. Felber and G. N. Pavlakis (2009). "Secretion and biological activity of short signal peptide IL-15 is chaperoned by IL-15 receptor alpha in vivo." J Immunol **183**(5): 3064-3072.
3. Bergamaschi, C., M. Rosati, R. Jalah, A. Valentin, V. Kulkarni, C. Alicea, G. M. Zhang, V. Patel, B. K. Felber and G. N. Pavlakis (2008). "Intracellular interaction of interleukin-15 with its receptor alpha during production leads to mutual stabilization and increased bioactivity." J Biol Chem **283**(7): 4189-4199.
4. Boyman, O., C. Krieg, D. Homann and J. Sprent (2012). "Homeostatic maintenance of T cells and natural killer cells." Cell Mol Life Sci **69**(10): 1597-1608.
5. Burke, S. J., D. Lu, T. E. Sparer, T. Masi, M. R. Goff, M. D. Karlstad and J. J. Collier (2014). "NF-kappaB and STAT1 control CXCL1 and CXCL2 gene transcription." Am J Physiol Endocrinol Metab **306**(2): E131-149.
6. Burkett, P. R., R. Koka, M. Chien, S. Chai, D. L. Boone and A. Ma (2004). "Coordinate expression and trans presentation of interleukin (IL)-15Ralpha and IL-15 supports natural killer cell and memory CD8+ T cell homeostasis." J Exp Med **200**(7): 825-834.
7. Burkett, P. R., R. Koka, M. Chien, S. Chai, F. Chan, A. Ma and D. L. Boone (2003). "IL-15R alpha expression on CD8+ T cells is dispensable for T cell memory." Proc Natl Acad Sci U S A **100**(8): 4724-4729.
8. Chenoweth, M. J., M. F. Mian, N. G. Barra, T. Alain, N. Sonenberg, J. Bramson, B. D. Lichty, C. D. Richards, A. Ma and A. A. Ashkar (2012). "IL-15 Can Signal

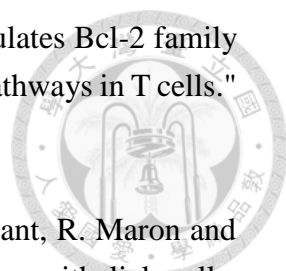
via IL-15R alpha, JNK, and NF-kappa B To Drive RANTES Production by Myeloid Cells." Journal of Immunology **188**(9): 4149-4157.

9. Chertova, E., C. Bergamaschi, O. Chertov, R. Sowder, J. Bear, J. D. Roser, R. K. Beach, J. D. Lifson, B. K. Felber and G. N. Pavlakis (2013). "Characterization and favorable in vivo properties of heterodimeric soluble IL-15.IL-15Ralpha cytokine compared to IL-15 monomer." J Biol Chem **288**(25): 18093-18103.
10. Cregg, J. M. and D. R. Higgins (1995). "Production of Foreign Proteins in the Yeast *Pichia-Pastoris*." Canadian Journal of Botany-Revue Canadienne De Botanique **73**: S891-S897.
11. Dann, S. M., H. C. Wang, K. J. Gambarin, J. K. Actor, P. Robinson, D. E. Lewis, S. Caillat-Zucman and A. C. White, Jr. (2005). "Interleukin-15 activates human natural killer cells to clear the intestinal protozoan cryptosporidium." J Infect Dis **192**(7): 1294-1302.
12. DePaolo, R. W., V. Abadie, F. Tang, H. Fehlner-Peach, J. A. Hall, W. Wang, E. V. Marietta, D. D. Kasarda, T. A. Waldmann, J. A. Murray, C. Semrad, S. S. Kupfer, Y. Belkaid, S. Guandalini and B. Jabri (2011). "Co-adjutant effects of retinoic acid and IL-15 induce inflammatory immunity to dietary antigens." Nature **471**(7337): 220-224.
13. Dragosits, M., J. Stadlmann, J. Albiol, K. Baumann, M. Maurer, B. Gasser, M. Sauer, F. Altmann, P. Ferrer and D. Mattanovich (2009). "The effect of temperature on the proteome of recombinant *Pichia pastoris*." J Proteome Res **8**(3): 1380-1392.
14. Dubois, S., J. Mariner, T. A. Waldmann and Y. Tagaya (2002). "IL-15Ralpha recycles and presents IL-15 In trans to neighboring cells." Immunity **17**(5): 537-547.
15. Fehniger, T. A. and M. A. Caligiuri (2001). "Interleukin 15: biology and relevance to human disease." Blood **97**(1): 14-32.
16. Friedmann, M. C., T. S. Migone, S. M. Russell and W. J. Leonard (1996). "Different interleukin 2 receptor beta-chain tyrosines couple to at least two signaling pathways and synergistically mediate interleukin 2-induced proliferation." Proc Natl Acad Sci U S A **93**(5): 2077-2082.

- 
17. Giri, J. G., S. Kumaki, M. Ahdieh, D. J. Friend, A. Loomis, K. Shanebeck, R. DuBose, D. Cosman, L. S. Park and D. M. Anderson (1995). "Identification and cloning of a novel IL-15 binding protein that is structurally related to the alpha chain of the IL-2 receptor." EMBO J **14**(15): 3654-3663.
18. Haan, C., C. Rolvering, F. Raulf, M. Kapp, P. Druckes, G. Thoma, I. Behrmann and H. G. Zerwes (2011). "Jak1 Has a Dominant Role over Jak3 in Signal Transduction through gamma c-Containing Cytokine Receptors." Chemistry & Biology **18**(3): 314-323.
19. Hsieh, C. S., S. E. Macatonia, C. S. Tripp, S. F. Wolf, A. O'Garra and K. M. Murphy (1993). "Development of TH1 CD4+ T cells through IL-12 produced by Listeria-induced macrophages." Science **260**(5107): 547-549.
20. Imamichi, H., I. Sereti and H. C. Lane (2008). "IL-15 acts as a potent inducer of CD4(+)CD25(hi) cells expressing FOXP3." Eur J Immunol **38**(6): 1621-1630.
21. Jabri, B. and V. Abadie (2015). "IL-15 functions as a danger signal to regulate tissue-resident T cells and tissue destruction." Nat Rev Immunol **15**(12): 771-783.
22. Koka, R., P. R. Burkett, M. Chien, S. Chai, F. Chan, J. P. Lodolce, D. L. Boone and A. Ma (2003). "Interleukin (IL)-15R[alpha]-deficient natural killer cells survive in normal but not IL-15R[alpha]-deficient mice." J Exp Med **197**(8): 977-984.
23. Lai, Y. G., M. S. Hou, A. Lo, S. T. Huang, Y. W. Huang, H. F. Yang-Yen and N. S. Liao (2013). "IL-15 modulates the balance between Bcl-2 and Bim via a Jak3/1-PI3K-Akt-ERK pathway to promote CD8 alpha alpha(+) intestinal intraepithelial lymphocyte survival." European Journal of Immunology **43**(9): 2305-2316.
24. Lawrence, T. (2009). "The nuclear factor NF-kappaB pathway in inflammation." Cold Spring Harb Perspect Biol **1**(6): a001651.
25. Lee, T. L., M. L. Chang, Y. J. Lin, M. H. Tsai, Y. H. Chang, C. M. Chuang, Y. Chien, T. Sosinowski, C. H. Wang, Y. Y. Chen, C. K. Lee, J. S. Chen, L. F. Wang, J. T. Kung and C. C. Ku (2015). "An alternatively spliced IL-15 isoform modulates abrasion-induced keratinocyte activation." J Invest Dermatol **135**(5): 1329-1337.

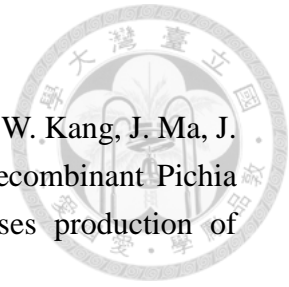
- 
26. Lodolce, J. P., P. R. Burkett, R. M. Koka, D. L. Boone and A. Ma (2002). "Regulation of lymphoid homeostasis by interleukin-15." Cytokine Growth Factor Rev **13**(6): 429-439.
27. Maley, F., R. B. Trimble, A. L. Tarentino and T. H. Plummer, Jr. (1989). "Characterization of glycoproteins and their associated oligosaccharides through the use of endoglycosidases." Anal Biochem **180**(2): 195-204.
28. Mathes, E., E. L. O'Dea, A. Hoffmann and G. Ghosh (2008). "NF-kappaB dictates the degradation pathway of IkappaBalpha." EMBO J **27**(9): 1357-1367.
29. McDonald, P. P., M. P. Russo, S. Ferrini and M. A. Cassatella (1998). "Interleukin-15 (IL-15) induces NF-kappa B activation and IL-8 production in human neutrophils." Blood **92**(12): 4828-4835.
30. Mishra, A., L. Sullivan and M. A. Caligiuri (2014). "Molecular Pathways: Interleukin-15 Signaling in Health and in Cancer." Clinical Cancer Research **20**(8): 2044-2050.
31. Napetschnig, J. and H. Wu (2013). "Molecular Basis of NF-kappa B Signaling." Annual Review of Biophysics, Vol 42 **42**: 443-468.
32. Obermeier, F., M. Hausmann, S. Kellermeier, S. Kiessling, U. G. Strauch, E. Duitman, S. Bulfone-Paus, H. Herfarth, J. Bock, N. Dunger, M. Stoeck, J. Scholmerich, W. Falk and G. Rogler (2006). "IL-15 protects intestinal epithelial cells." Eur J Immunol **36**(10): 2691-2699.
33. Ohteki, T., K. Suzue, C. Maki, T. Ota and S. Koyasu (2001). "Critical role of IL-15-IL-15R for antigen-presenting cell functions in the innate immune response." Nat Immunol **2**(12): 1138-1143.
34. Olsen, S. K., N. Ota, S. Kishishita, M. Kukimoto-Niino, K. Murayama, H. Uchiyama, M. Toyama, T. Terada, M. Shirouzu, O. Kanagawa and S. Yokoyama (2007). "Crystal Structure of the interleukin-15.interleukin-15 receptor alpha complex: insights into trans and cis presentation." J Biol Chem **282**(51): 37191-37204.
35. Pandiyan, P., X. P. Yang, S. S. Saravanamuthu, L. Zheng, S. Ishihara, J. J. O'Shea

- and M. J. Lenardo (2012). "The role of IL-15 in activating STAT5 and fine-tuning IL-17A production in CD4 T lymphocytes." J Immunol **189**(9): 4237-4246.
36. Perera, P. Y., J. H. Lichy, T. A. Waldmann and L. P. Perera (2012). "The role of interleukin-15 in inflammation and immune responses to infection: implications for its therapeutic use." Microbes Infect **14**(3): 247-261.
37. Rausch, A., M. Hessmann, A. Holscher, T. Schreiber, S. Bulfone-Paus, S. Ehlers and C. Holscher (2006). "Interleukin-15 mediates protection against experimental tuberculosis: a role for NKG2D-dependent effector mechanisms of CD8+ T cells." Eur J Immunol **36**(5): 1156-1167.
38. Ring, A. M., J. X. Lin, D. Feng, S. Mitra, M. Rickert, G. R. Bowman, V. S. Pande, P. Li, I. Moraga, R. Spolski, E. Ozkan, W. J. Leonard and K. C. Garcia (2012). "Mechanistic and structural insight into the functional dichotomy between IL-2 and IL-15." Nat Immunol **13**(12): 1187-1195.
39. Romanos, M. A., C. A. Scorer and J. J. Clare (1992). "Foreign Gene-Expression in Yeast - a Review." Yeast **8**(6): 423-488.
40. Ruckert, R., K. Asadullah, M. Seifert, V. M. Budagian, R. Arnold, C. Trombotto, R. Paus and S. Bulfone-Paus (2000). "Inhibition of keratinocyte apoptosis by IL-15: a new parameter in the pathogenesis of psoriasis?" J Immunol **165**(4): 2240-2250.
41. Sandau, M. M., K. S. Schluns, L. Lefrancois and S. C. Jameson (2004). "Cutting edge: transpresentation of IL-15 by bone marrow-derived cells necessitates expression of IL-15 and IL-15R alpha by the same cells." J Immunol **173**(11): 6537-6541.
42. Sato, N., H. J. Patel, T. A. Waldmann and Y. Tagaya (2007). "The IL-15/IL-15Ralpha on cell surfaces enables sustained IL-15 activity and contributes to the long survival of CD8 memory T cells." Proc Natl Acad Sci U S A **104**(2): 588-593.
43. Schluns, K. S., W. C. Kieper, S. C. Jameson and L. Lefrancois (2000). "Interleukin-7 mediates the homeostasis of naive and memory CD8 T cells in vivo." Nat Immunol **1**(5): 426-432.

- 
44. Shenoy, A. R., S. Kirschnek and G. Hacker (2014). "IL-15 regulates Bcl-2 family members Bim and Mcl-1 through JAK/STAT and PI3K/AKT pathways in T cells." European Journal of Immunology **44**(8): 2500-2507.
45. Shinozaki, M., J. Hirahashi, T. Lebedeva, F. Y. Liew, D. J. Salant, R. Maron and V. R. Kelley (2002). "IL-15, a survival factor for kidney epithelial cells, counteracts apoptosis and inflammation during nephritis." J Clin Invest **109**(7): 951-960.
46. Stone, K. P., A. J. Kastin and W. H. Pan (2011). "NF kappa B is an Unexpected Major Mediator of Interleukin-15 Signaling in Cerebral Endothelia." Cellular Physiology and Biochemistry **28**(1): 115-124.
47. Stonier, S. W. and K. S. Schluns (2010). "Trans-presentation: A novel mechanism regulating IL-15 delivery and responses." Immunology Letters **127**(2): 85-92.
48. Sun, W., Y. Lai, H. Li, T. Nie, Y. Kuang, X. Tang, K. Li, P. R. Dunbar, A. Xu, P. Li and D. Wu (2016). "High level expression and purification of active recombinant human interleukin-15 in *Pichia pastoris*." J Immunol Methods **428**: 50-57.
49. Tan, X. and L. Lefrancois (2006). "Novel IL-15 isoforms generated by alternative splicing are expressed in the intestinal epithelium." Genes and Immunity **7**(5): 407-416.
50. Viatour, P., M. P. Merville, V. Bours and A. Chariot (2005). "Phosphorylation of NF-kappa B and I kappa B proteins: implications in cancer and inflammation." Trends in Biochemical Sciences **30**(1): 43-52.
51. Waldmann, T. A. (2006). "The biology of interleukin-2 and interleukin-15: implications for cancer therapy and vaccine design." Nat Rev Immunol **6**(8): 595-601.
52. Yang, S., Y. Kuang, H. Li, Y. Liu, X. Hui, P. Li, Z. Jiang, Y. Zhou, Y. Wang, A. Xu, S. Li, P. Liu and D. Wu (2013). "Enhanced production of recombinant secretory proteins in *Pichia pastoris* by optimizing Kex2 P1' site." PLoS One **8**(9): e75347.
53. Zhao, Y. M. and A. R. French (2013). "Mechanistic model of natural killer cell proliferative response to IL-15 receptor stimulation." PLoS Comput Biol **9**(9):

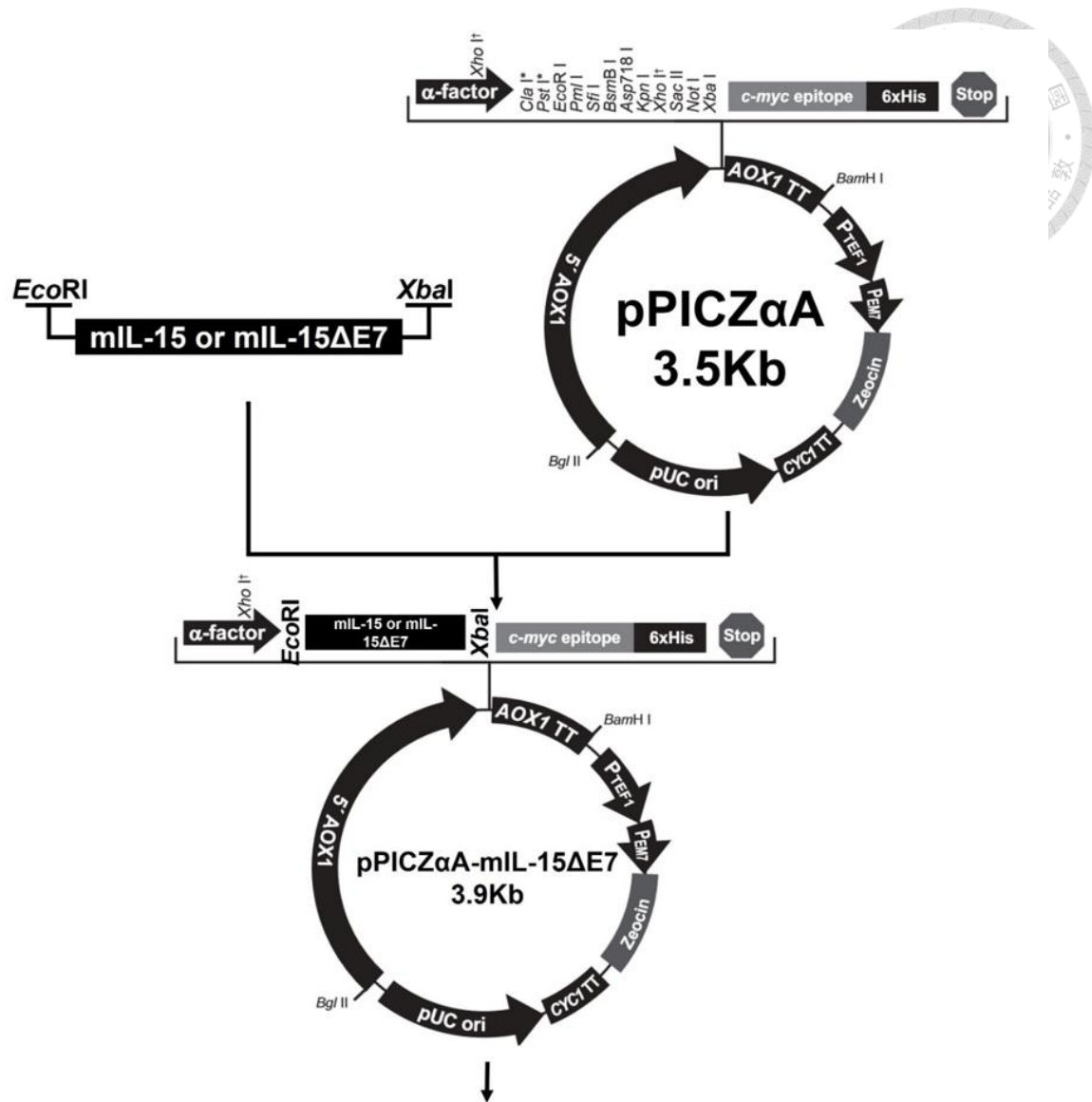
e1003222.

54. Zhong, Y., L. Yang, Y. Guo, F. Fang, D. Wang, R. Li, M. Jiang, W. Kang, J. Ma, J. Sun and W. Xiao (2014). "High-temperature cultivation of recombinant *Pichia pastoris* increases endoplasmic reticulum stress and decreases production of human interleukin-10." Microb Cell Fact **13**: 163.





Figures



Transformation into the *Pichia* Strain

Figure 1. Generation of recombinant IL-15 and IL-15ΔE7 from *Pichia* expression system

Mouse IL-15 or IL-15ΔE7 gene flanked with FLAG were cloned from pEF-mIL-15(FLAG) or pEF-mIL-15ΔE7(FLAG) by PCR, respectively. *EcoRI* and *XbaI* restriction enzyme sites were also introduced into these two genes by PCR. PCR products and pPICZ α A were then digested by *EcoRI* and *XbaI*, followed by ligation of digested PCR products to digested pPICZ α A. Constructed pPICZ α A-mIL-15 or pPICZ α A-mIL-15ΔE7 was then transformed into X-33 strain to generate mouse IL-15 or IL-15ΔE7 expressing yeast.

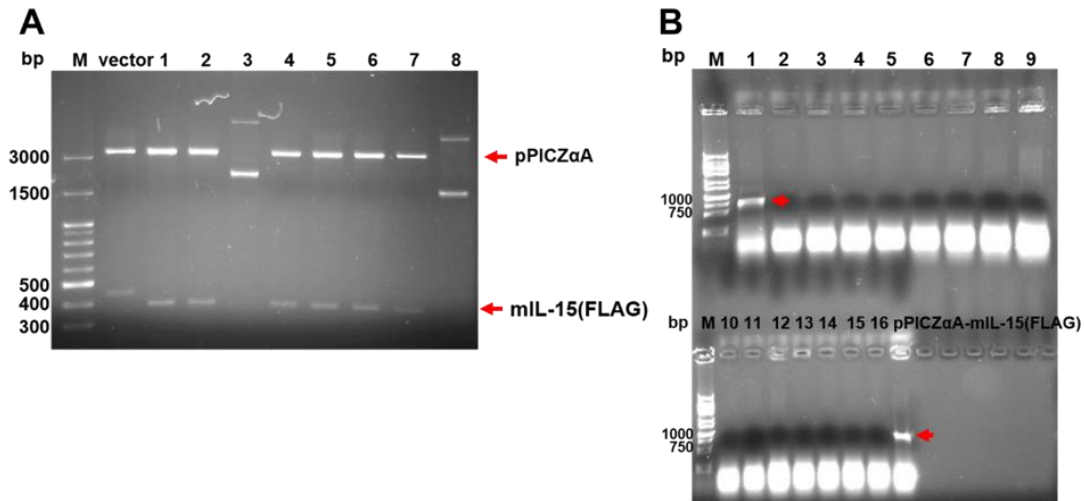


Figure 2. Verification of IL-15 and IL-15 Δ E7 construct using restriction enzyme digestion and colony PCR

(A) Bacterial colonies from IL-15-pPICZ α A transformed *E. coli* were picked and grown in 3mL LB medium overnight. Plasmid DNA (1ug) extracted from each transformant digested with *Eco*RI and *Xba*I and resolved on 0.8% agarose gel by electrophoresis. The arrows indicated pPICZ α A and (3100 bp) mIL-15(FLAG) (380 bp) fragments, individually.

(B) Bacterial colonies from IL-15 Δ E7-pPICZ α A transformed *E. coli* were resuspended in 20 uL LB medium. Transformants that contained IL-15 Δ E7 were screened by PCR using 5'AOX1 and 3'AOX1 primer set. IL-15-pPICZ α A construct was included as positive control. PCR product (850 bp) was resolved on 0.8% agarose gel by electrophoresis.

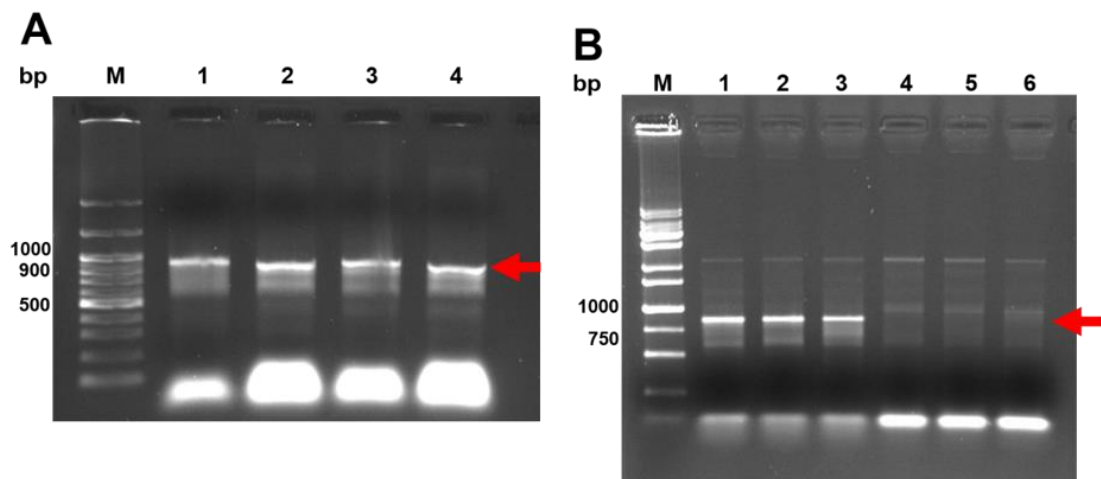


Figure 3. Genotyping of IL-15 and IL-15 Δ E7 transformed X-33 strain

Yeast X-33 strain was transformed with from IL-15-pPICZ α A (A) or IL-15 Δ E7-pPICZ α A (B) and grown on Yeast Extraction Dextrose (YPD) agar plates. Transformed X-33 colonies were picked and resuspended in YPD medium and analyzed by PCR using 5'AOX1 and 3'AOX1 primer set. PCR product (IL-15: 850 bp, IL-15 Δ E7: 800 bp) resolved on the 0.8% agarose gel by electrophoresis. The arrows indicated correct PCR products.

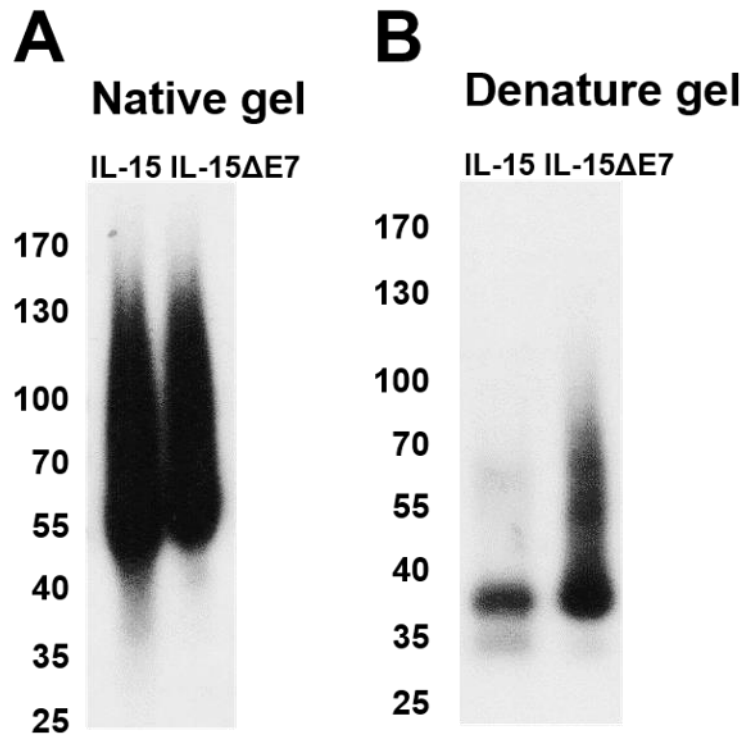


Figure 4. Western blot analysis of purified yeast recombinant IL-15 and IL-15 Δ E7 (A) 500 ng of IL-15 or IL-15 Δ E7 was resuspended in sample buffer without denaturing reagent (β -mercaptoethanol) (A) or with 1% β -mercaptoethanol (B) and then resolved on a (4% to 20%) gradient SDS-PAGE. by electrophoresis. Expression of IL-15 or IL-15 Δ E7 was detected by anti-IL-15 antibody by Western blot analysis. The molecular weight of denatured IL-15 or IL-15 Δ E7 is about 36 kDa.

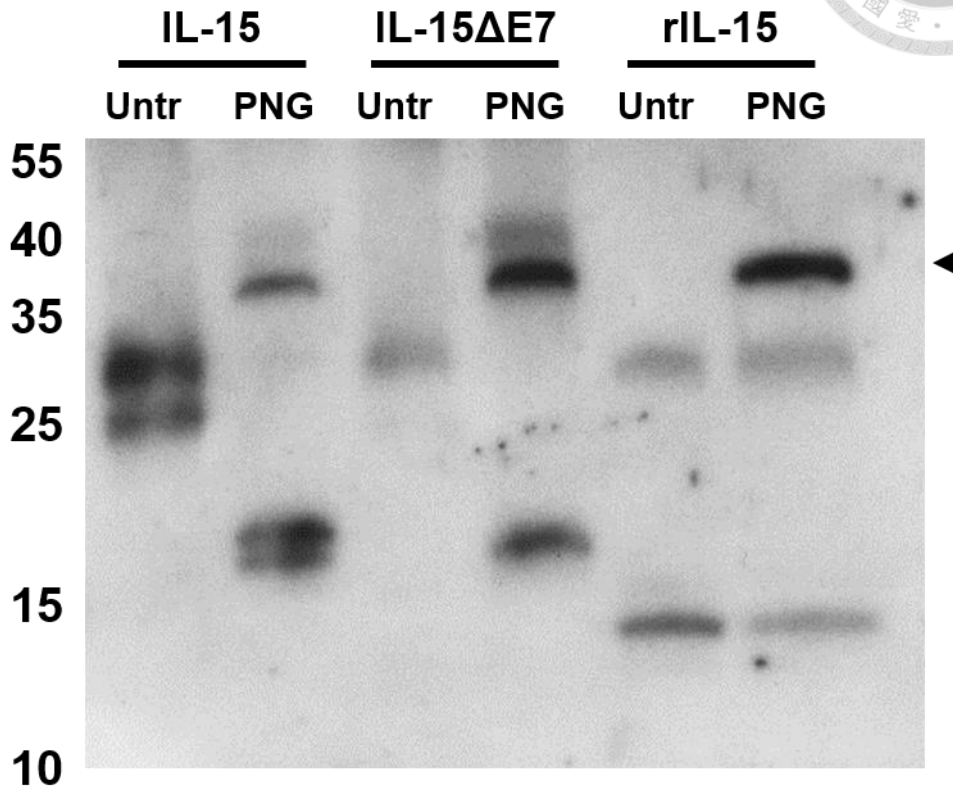
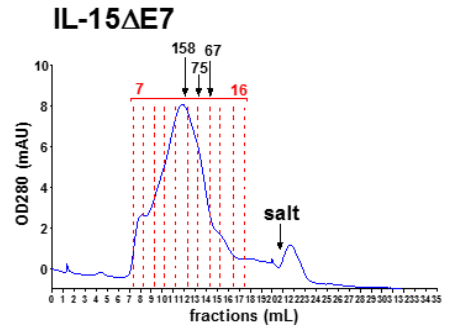
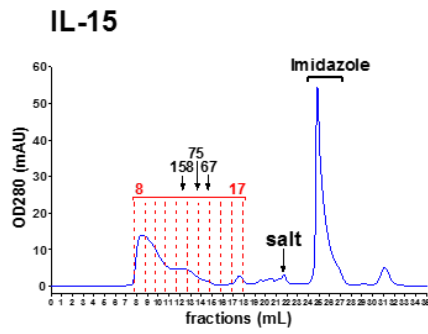


Figure 5. Western blot analysis of deglycosylated IL-15 and IL-15ΔE7

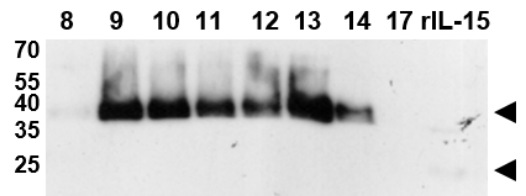
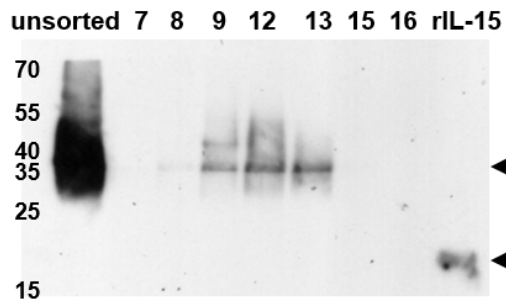
200 ng of yeast IL-15, IL-15ΔE7 or commercially purchased, *E.coli* derived recombinant IL-15 (Shenandoah Inc.) was denatured in 1% β-ME followed by the treatment with PNGase F for deglycosylation. Deglycosylated protein (PNG) was resuspended in sample buffer and then resolved on a 15% SDS-PAGE by electrophoresis for Western blot analysis by anti-IL-15 antibody. Same protein which was not treated with PNGase F (Untr) was analyzed in parallel. The molecular weights of untreated and PNGase F-treated yeast IL-15 and IL-15ΔE7 are about 35 kDa and 17 kDa, respectively. Those of untreated and PNGase F-treated *E.coli* IL-15 are about 13 kDa.



A



B



C

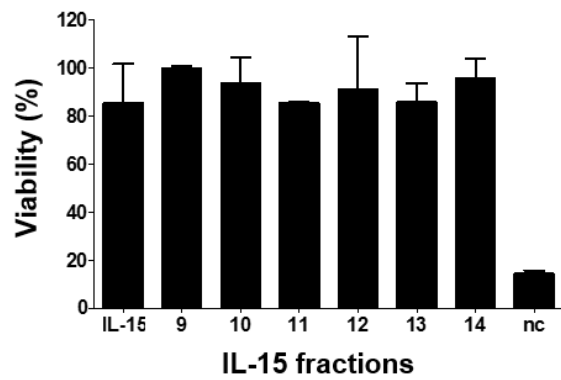


Figure 6. FPLC analysis of recombinant IL-15 and IL-15ΔE7 proteins prepared from yeast expression system

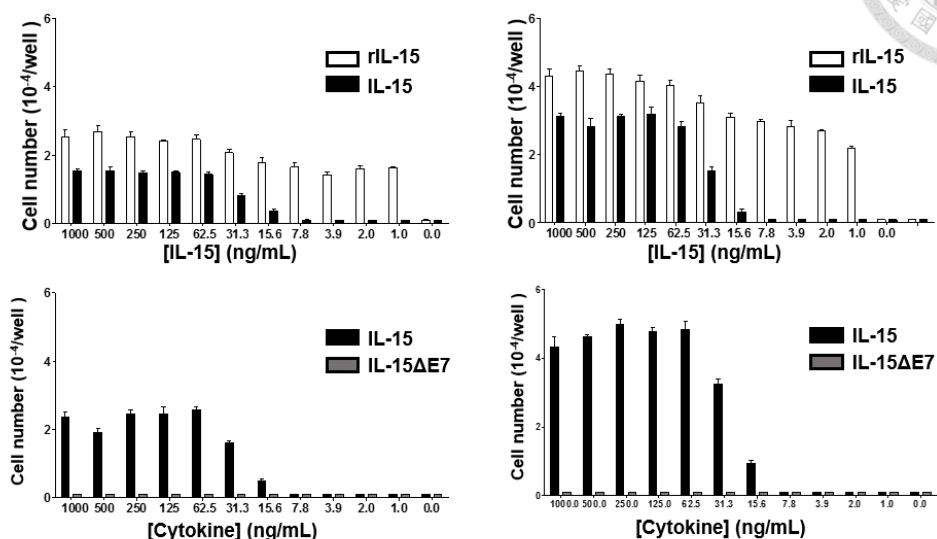
(A) Purified recombinant IL-15 and IL-15ΔE7 was separated with FPLC. Fractions 7-16 for IL-15 sample or fractions 8-17 for IL-15ΔE7 sample were collected for further analysis. The arrows indicate molecular weight (kDa). (B) Western blot analysis of FPLC fractions by anti-IL-15 antibody. The molecular weight of yeast expressing IL-15 and IL-15ΔE7 is about 35 kDa compared with purchased *E. coli* derived recombinant mouse IL-15 which is at about 13 kDa. (C) Washed HT-2 cells (4×10^4 cells/ml) were treated with yeast recombinant WT-IL-15 from FPLC fractions 9-14 overnight. The cell viability was then examined by MTT assay. Conversion of MTT compound from yellow solution to violet crystals by mitochondrial NAD(P)H-dependent cellular oxidoreductase in viable cells were measured at OD595 in an ELISA reader after dissolution of the crystals in acidic isopropanol solution. Each bar represents the mean \pm SEM derived from data of duplicate wells.



A

a. Beginning from 10^4 HT-2 cells

b. Beginning from 2×10^4 HT-2 cells



B

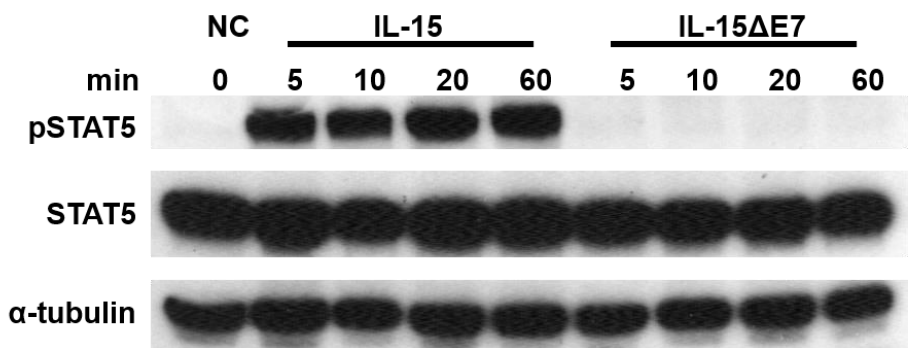


Figure 7. The cell viability and the phosphorylation of STAT5 in HT-2 cells after treated with yeast recombinant IL-15 and IL-15ΔE7

(A) HT-2 cells at 1×10^5 cells/ml (a) or at 2×10^5 cells/ml (b) were treated with various amount of yeast recombinant IL-15, IL-15ΔE7 or *E. coli* derived recombinant mouse IL-15 (rIL-15) for 24 h. The cell viability was examined by MTT assay as described in Figure 5C. Each bar represents the mean \pm SEM derived from data of triplicate wells.

(B) Starved HT-2 cells (1×10^6 cells/ml) were treated with IL-15 or IL-15ΔE7 at 150 ng/mL. Protein lysates were collected at treatment 5, 10, 20, and 60 min after treatment. to analyze the Phosphorylation of STAT5 was analyzed by immunoblotting analysis using anti-phosphoSTAT5 antibody.

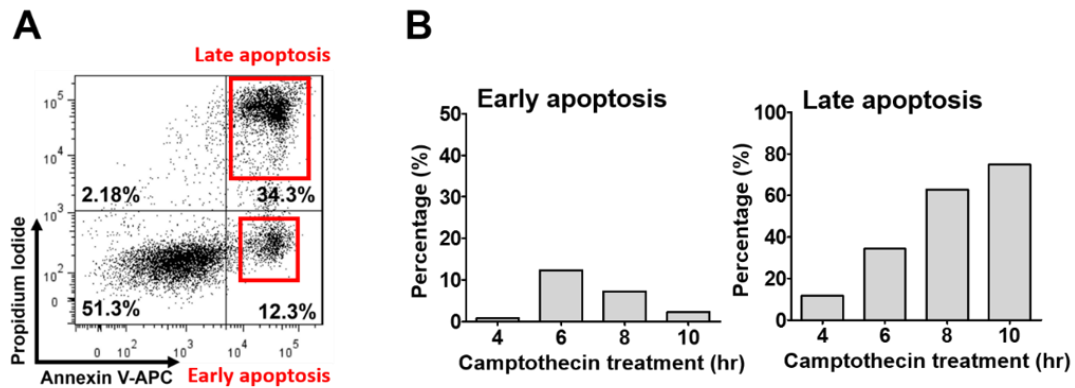
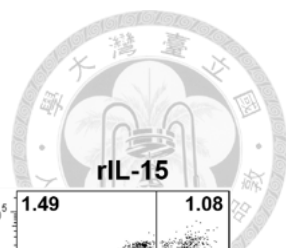
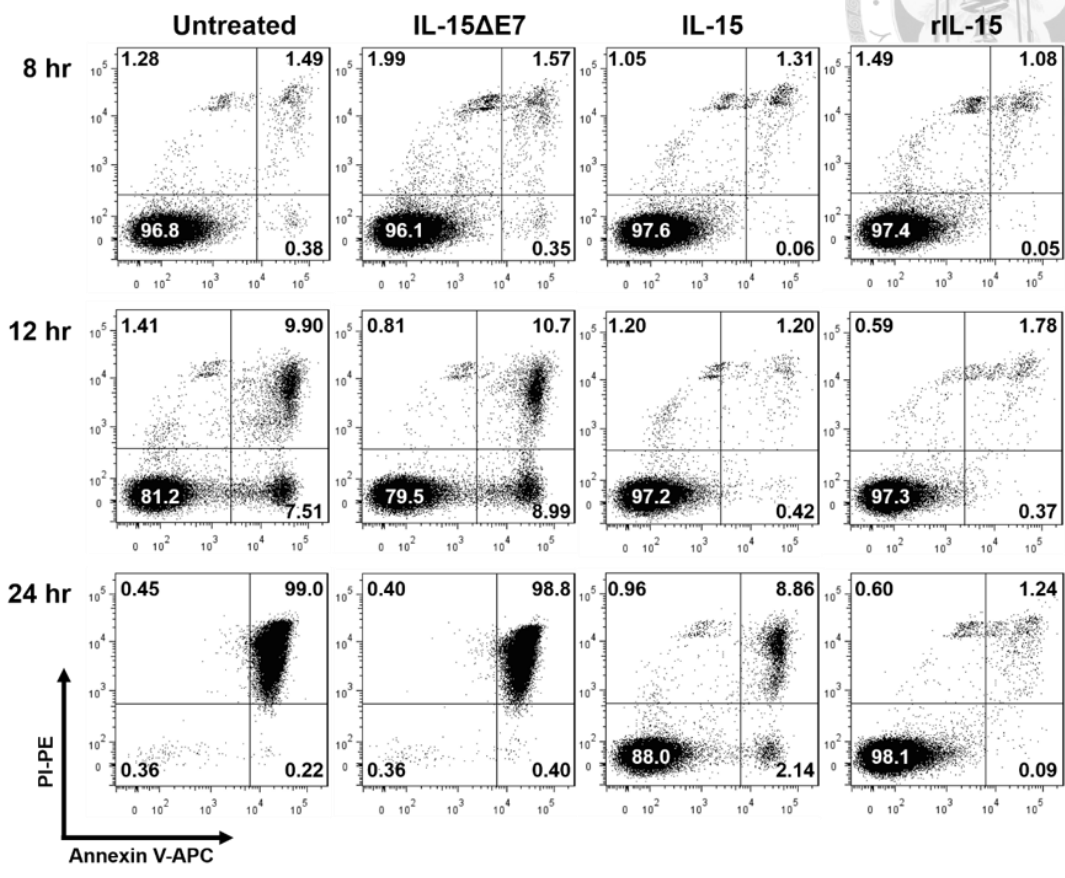


Figure 8. Induction of cell apoptosis in HT-2 cells by camptothecin treatment.

(A) HT-2 cells (1×10^6 cells/ml) were treated with 5 μ M of camptothecin. The cells at 4, 6, 8 and 10 hour post-treatment were stained with APC-conjugated Annexin V and propidium iodine (PI) for flow cytometric analysis. Cells that are stained with Annexin V but excludes PI dye are defined as early apoptosis; cells that are stained with both Annexin V and PI are defined as late apoptosis. The percentages of camptothecin-induced cell apoptosis at early stage or at late stage at different time points were shown in panel B.



A



B

Annexin V⁺ apoptotic cells

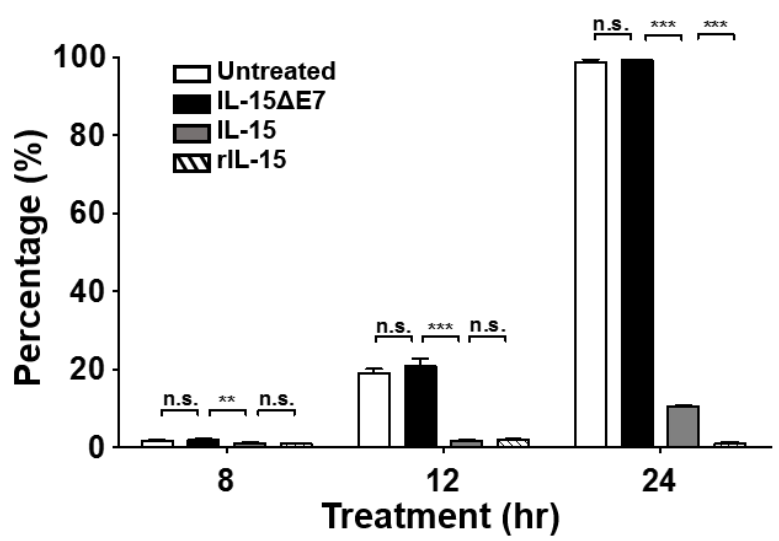


Figure 9. IL-15ΔE7 did not enhance apoptosis of cytokine-deprived HT-2 cells.

HT-2 cells (2×10^5 cells/ml) were left untreated or treated with yeast recombinant IL-15, IL-15ΔE7 or purchased mouse recombinant IL-15 at 150 ng/ml in a 24-well microtiter plate (1 mL/well) for 8, 12 and 24 hours. The cells were stained with APC-conjugated Annexin V and propidium iodine (PI) for flow cytometry as described in the legend of Figure 8. Representative dot plots for untreated, IL-15-treated, IL-15ΔE7-treated or rIL-15-treated HT-2 cells are shown in panel A. The percentages of Annexin V positive apoptotic HT-2 cells in untreated, IL-15-treated, IL-15ΔE7-treated or rIL-15-treated groups at different time points are shown in panel B. Each bar in panel B represents the mean \pm SEM derived from data of triplicate wells.

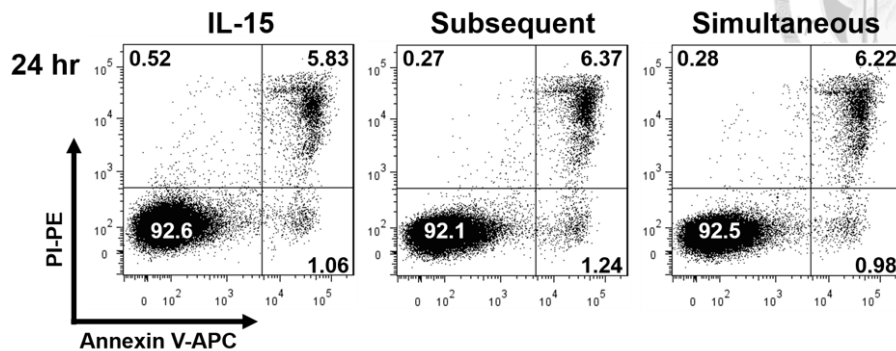
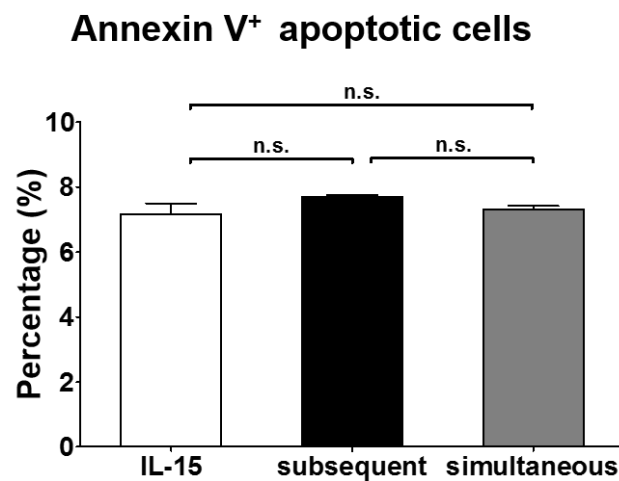
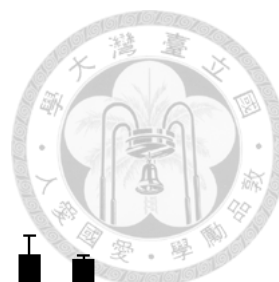
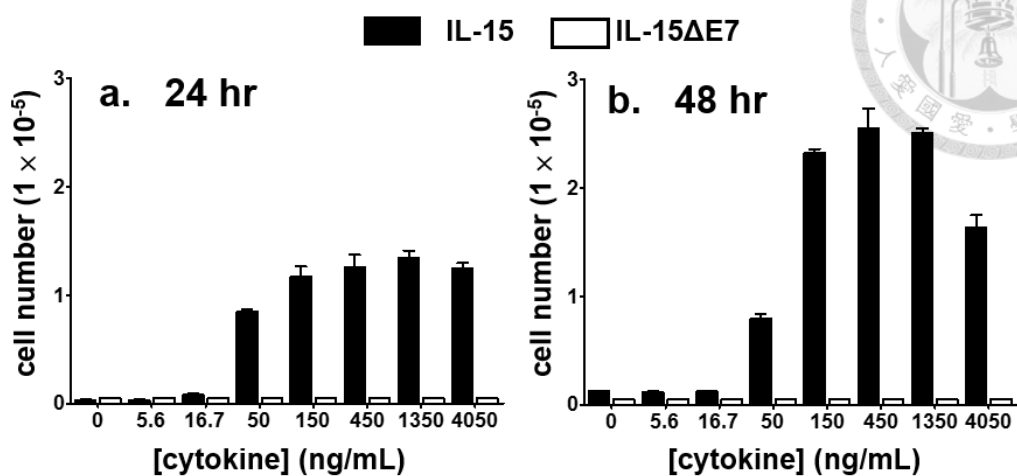
A**B**

Figure 10. IL-15ΔE7 did not affect IL-15 functions of cell survival maintenance and apoptosis inhibition.

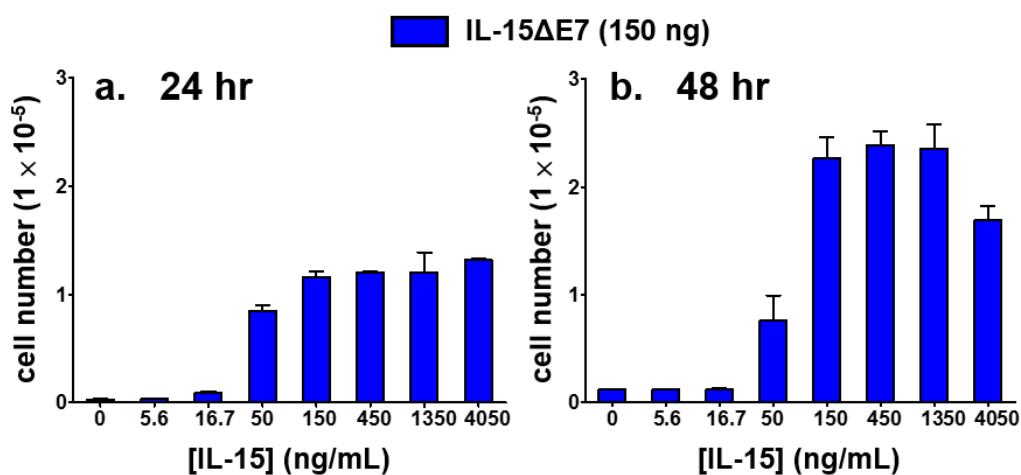
HT-2 cells (2×10^5 cells/ml) were pre-treated with IL-15ΔE7 for 1 hour, followed by IL-15 treatment (150 ng/mL), or treated with the mixture of equal amount of IL-15 and IL-15ΔE7 (150 ng/mL each) in a 24-well microtiter plate (1 mL/well). Cells that were treated with IL-15 alone (150 ng/mL) were used as the comparison group. The cells were then stained with APC-conjugated Annexin V and propidium iodine (PI) for flow cytometry as described in the legend of Figure 8. Representative dot plots for HT-2 cells with indicated treated protocol are shown in panel A. The percentages of Annexin V positive apoptotic HT-2 cells treated with IL-15 alone, subsequent treatment or simultaneous co-treatment at the 24 hour are shown in panel B. Each bar in panel B represents the mean \pm SEM derived from data of triplicate wells.



A. Single treatment



B. Co-treatment



C. Co-treatment

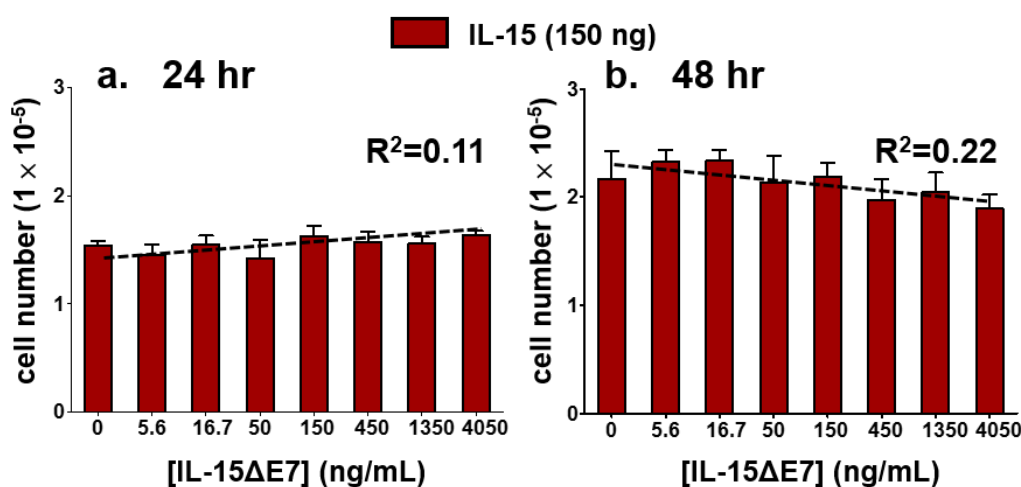
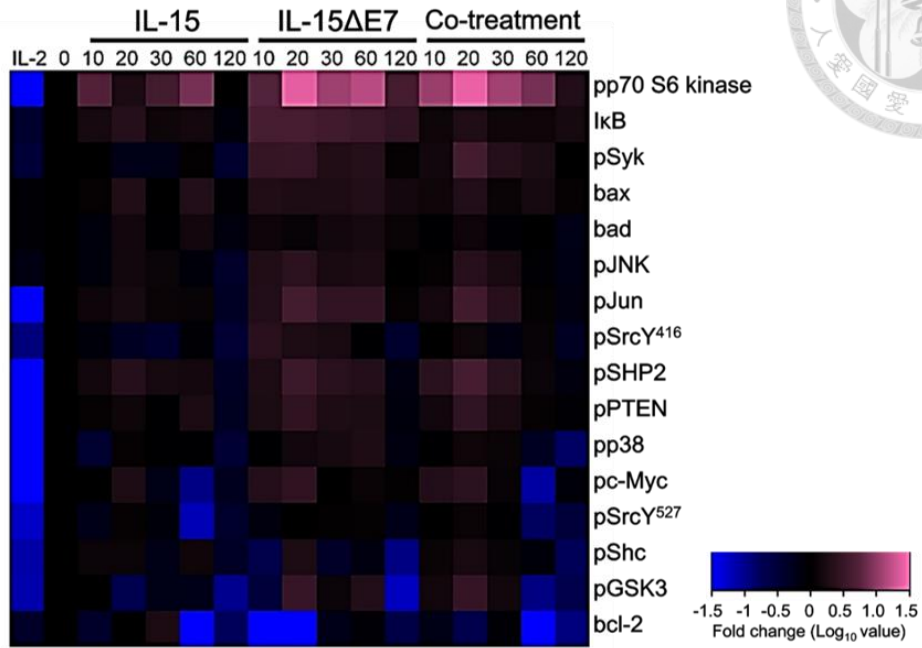


Figure 11. Exogenous addition of IL-15ΔE7 at all doses does not block IL-15-mediated HT-2 cell proliferation.

(A) HT-2 cells (1×10^5 cells/mL) were treated with various amount of yeast recombinant IL-15 or IL-15ΔE7 for 24 hours (a) and 48 hours (b). To investigate whether IL-15ΔE7 had inhibitory effect on IL-15-mediated cell proliferation, HT-2 cells (1×10^5 cells/mL) were either treated with a mixture of IL-15ΔE7 (150 ng/mL) and various amount of IL-15 (B) or treated with a mixture of IL-15 (150 ng/mL) with various amount of IL-15ΔE7 (C) for 24 hours (panel a) and 48 hours (panel b). Cell viability was determined by the mitochondrial dehydrogenase activities in living cells by colorimetric method-based MTT assays. The number of living cells was calculated by converting the absorbance reading from each well to absolute number using a standard curve. The reference standard curve was generated by measuring the absorbance at OD595 versus HT-2 cell number (starting from 1×10^6 to 1×10^4 by serial 2-fold dilution). Each bar represents the mean \pm SD derived from triplicate wells. Inhibition of IL-15 mediated cell proliferation by IL-15ΔE7 at various doses in Figure C was analyzed by regression analysis and the R^2 value was calculated accordingly. Shown in Figure A are representative results from two independent experiments. Shown in Figure B and Figure C are representative results from three similar experiments.



A



B

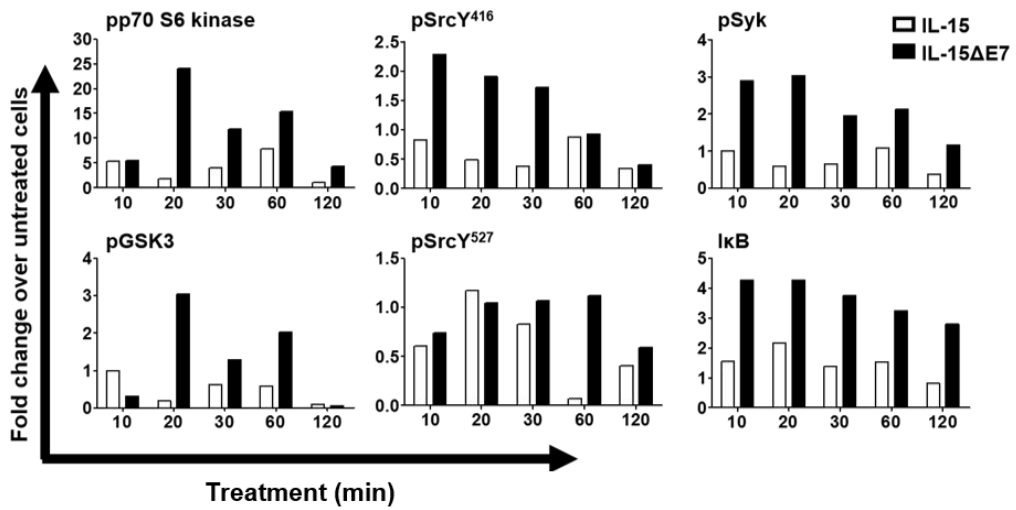


Figure 12. Signalosome profiles in IL-15 Δ E7-treated HT-2 cells by Micro-western analysis

Starved HT-2 cells were treated with IL-15/GST (10 nM), IL-15 Δ E7/GST (10 nM) or cotreatment (at 5:1 ratio). Protein lysates collected at various times were subjected to Micro-Western assay to profile the signaling activated in each group of cells. The expression level of each protein was normalized to untreated cells and the logarithmic value was computed by R program. (A) Signalosome profiles in IL-15, IL-15 Δ E7 or co-treated cells are presented in color coded heat map (-1.5 to 1.5; blue to purple). (B) Western blot analysis of selective signaling molecules identified from (A). Bars are expressed as fold change for the level of phosphorylation in treated cells compared to untreated control after normalization to α -tubulin. Micro-Western experiments were performed by Array core facility of National Health Research Institutes.

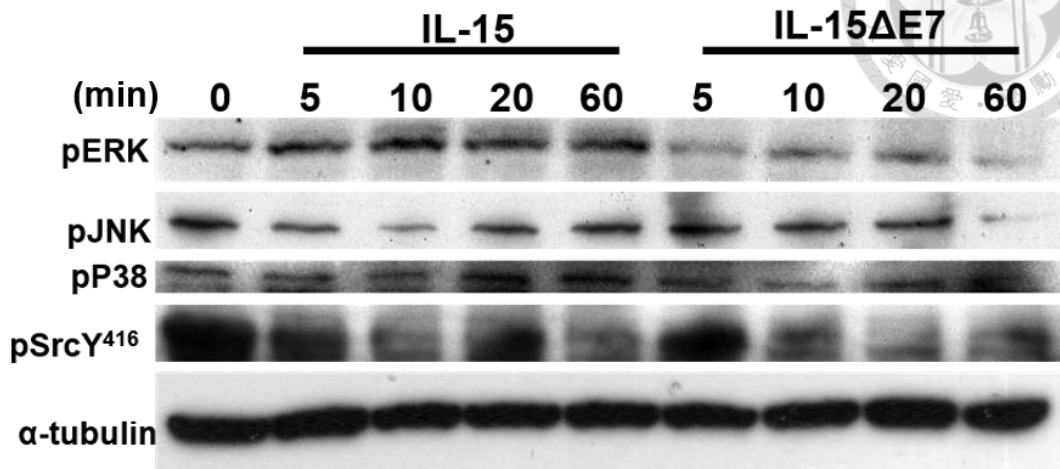
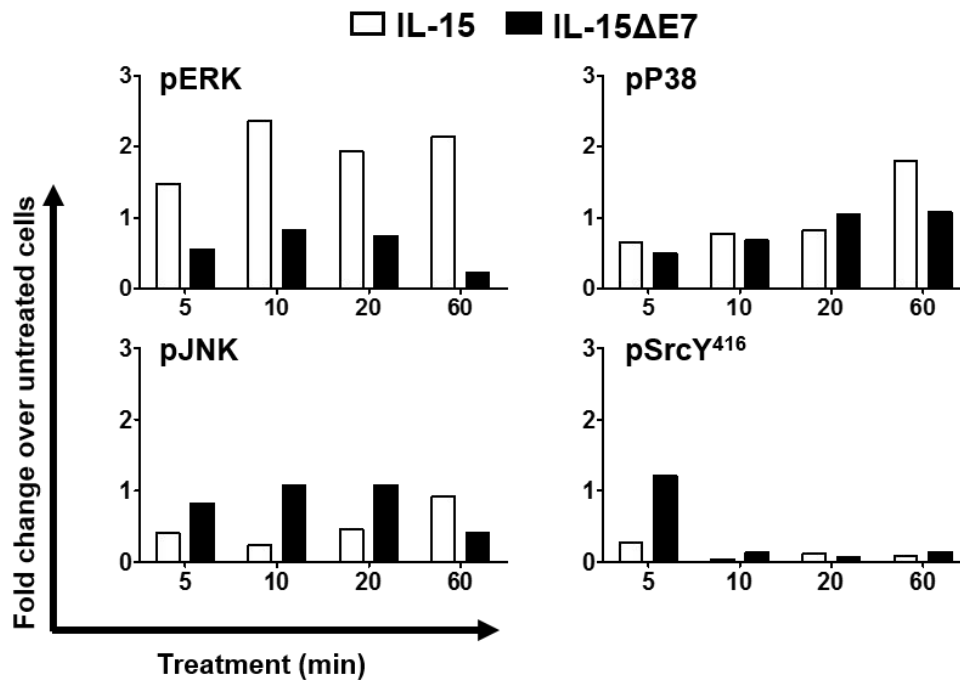
A**B**

Figure 13. Activation of Src and MAPK pathway by IL-15ΔE7

Starved HT-2 cells (1×10^6) were treated with yeast recombinant IL-15 or IL-15ΔE7 protein (150 ng/ml). (A) Cell lysate collected from as indicated times after cytokine treatment was analyzed for the phosphorylation of ERK, p38, JNK and SrcY⁴¹⁶ by Western blot analysis. (B) The phosphorylation levels of each protein were quantified by ImageJ program by measuring pixel intensity shown in (A). Data are expressed by fold change from untreated cells.

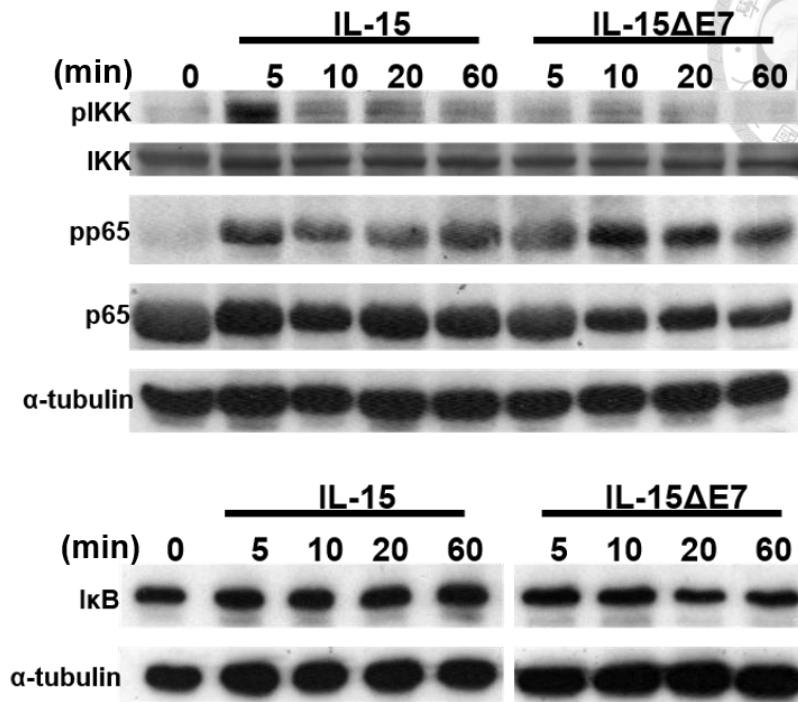
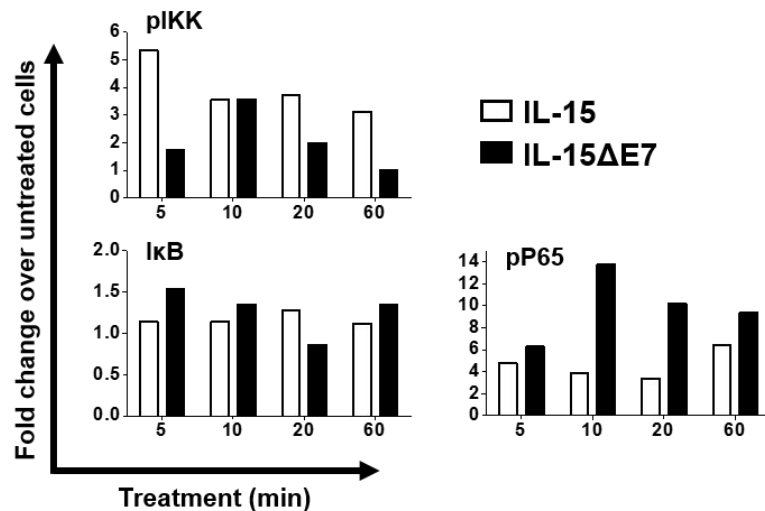
A**B**

Figure 14. IL-15ΔE7 treatment suppressed IKKαβ phosphorylation but enhanced p65 phosphorylation compared to IL15 treatment.

Starved HT-2 cells (1×10^6) were treated with yeast recombinant IL-15 or IL-15ΔE7 protein (150 ng/ml). (A) Phosphorylation of IKKαβ and p65 as well as total IkB was analyzed by immunoblots. (B) The phosphorylation levels of each protein were quantified by ImageJ program by measuring pixel intensity shown in (A). Data are expressed by fold change from untreated cells.

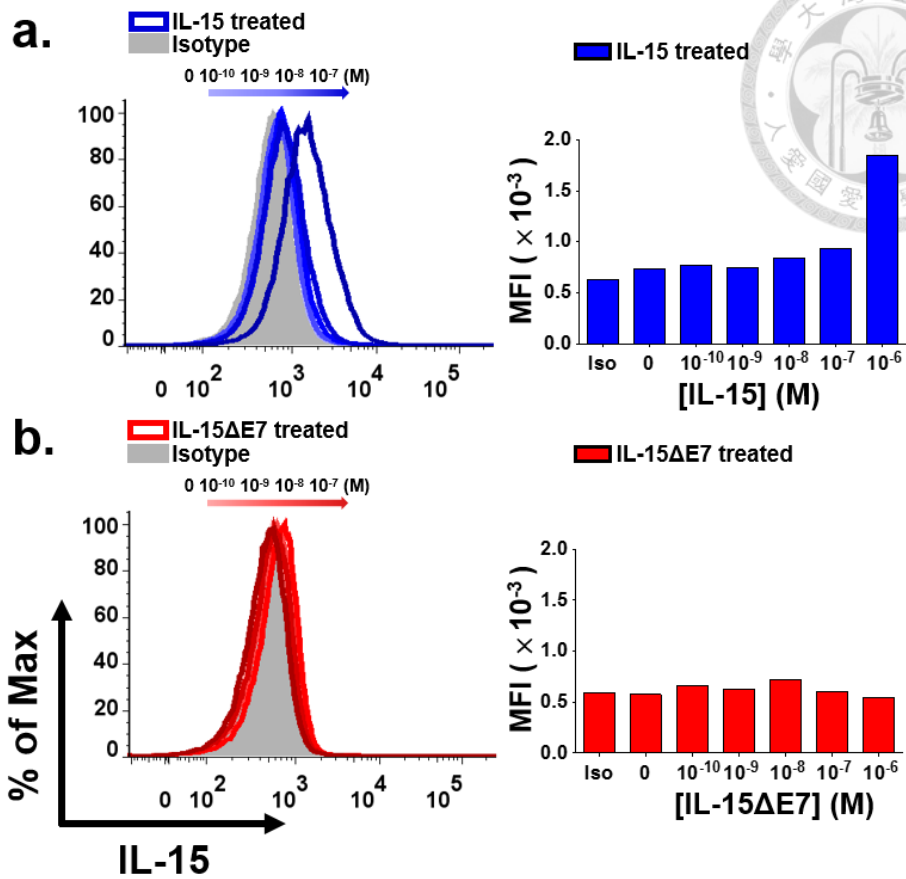
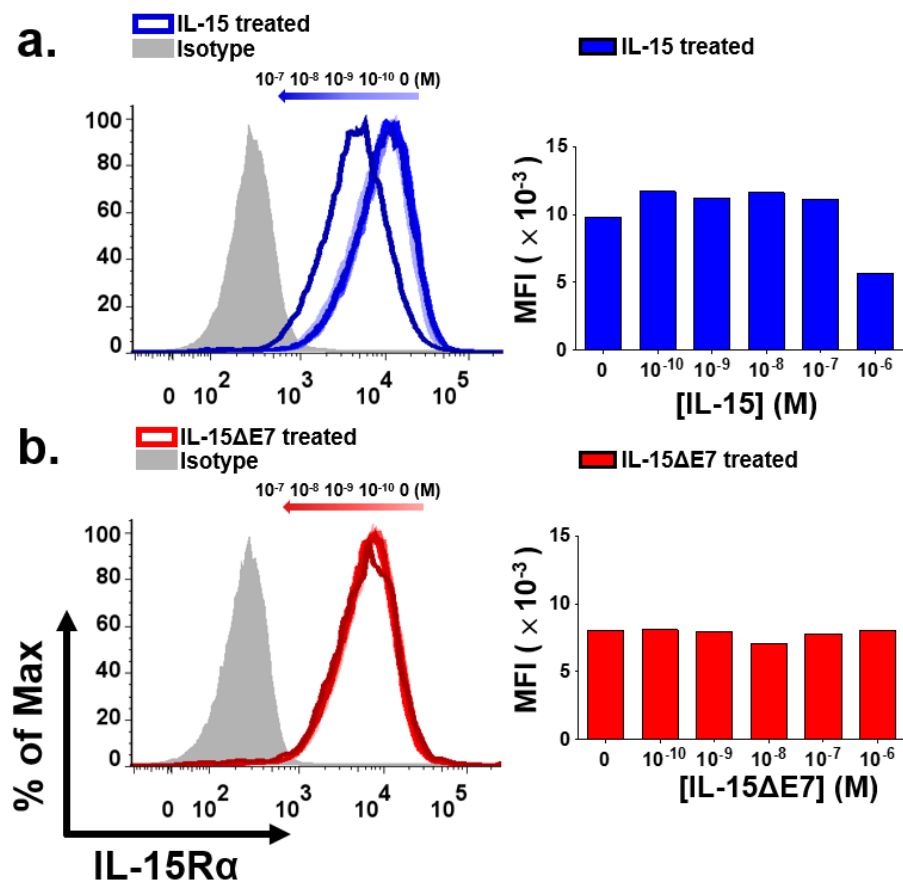
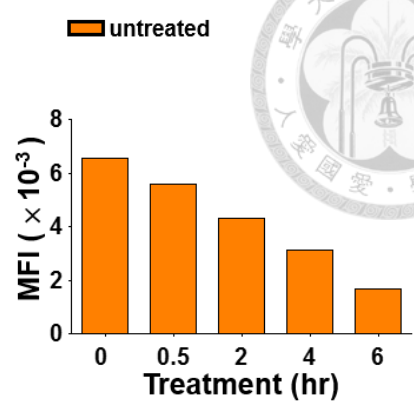
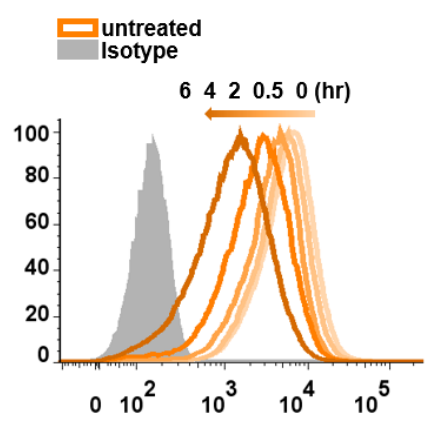
A**B**

Figure 15. Dose effects of IL-15 or IL-15ΔE7 on the surface expression of IL-15 or IL-15Rα in IL-15Rα-COS-7 cells

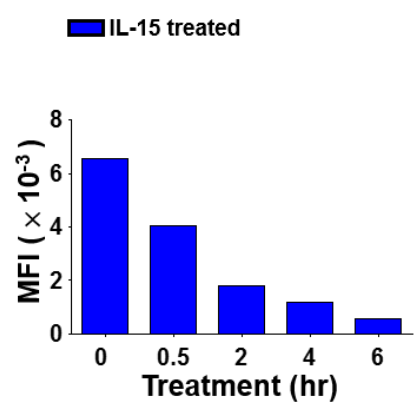
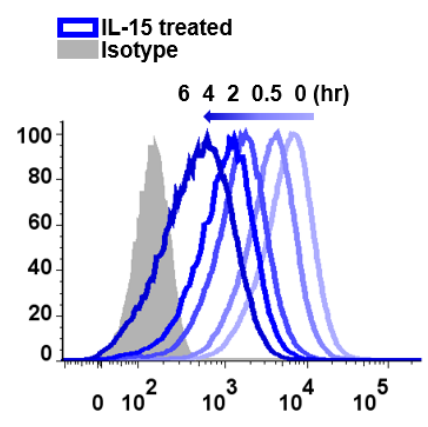
Dislodged IL-15Rα-COS-7 cells (1×10^6 cells/mL) were treated with IL-15 or IL-15ΔE7 at 10^{-7} , 10^{-8} , 10^{-9} or 10^{-10} M and incubated on ice for 2 hours. The cells were stained with either goat anti-IL-15 (A) or goat anti-IL-15Rα polyclonal Ab (B) followed by incubation with biotinylated secondary anti-goat antibody. Biotinylated antibody was detected with streptavidin-conjugated APC fluorochrome and analyzed by flow cytometry. GFP positive and propidium iodide negative cells were gated for live IL-15Rα-COS-7 cells. Results shown are histogram profiles of IL-15 (A) or IL-15Rα (B) staining of IL-15Rα-COS-7 cells treated with increasing concentrations of IL-15 (panel a, blue lines) or IL-15ΔE7 (panel b, red lines). Bar charts shown on the right are the mean fluorescence intensity (MFI) of IL-15 staining in IL-15-treated (blue bars) or IL-15ΔE7-treated (red bars) IL-15Rα-COS-7 cells at each concentration. Background (shown in grey) was the fluorescence profile of untreated IL-15Rα-COS-7 cells stained with isotype control antibody.



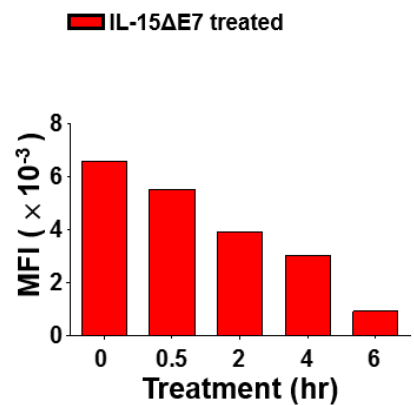
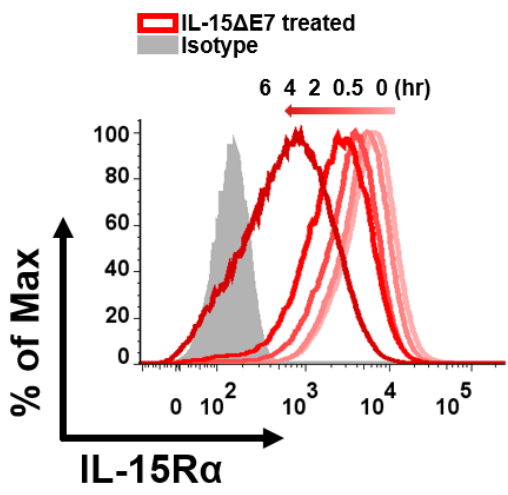
A



B



C



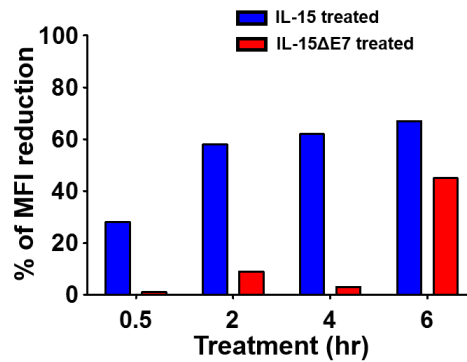
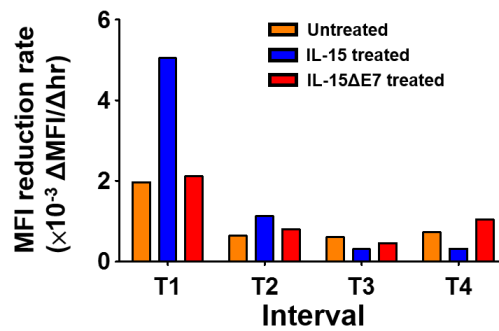
D**E**

Figure 16. Temporal expression of IL-15R α in IL-15R α -COS-7 cells after treated with IL-15 or IL-15 Δ E7

Dislodged IL-15R α -COS-7 cells (1×10^6 cells/mL) were left untreated, or treated with IL-15 (10^{-7} M) or IL-15 Δ E7 (10^{-7} M) for 0, 0.5, 2, 4 and 6 hours at 37°C . At each time point, cells were harvested and stained with goat anti-IL-15R α polyclonal antibody as described in the legend of Figure 15. Results shown are histogram profiles of IL-15R α staining in IL-15R α -COS-7 cells which were left untreated (A), IL-15-treated (B) or IL-15 Δ E7-treated (C) for indicated times. Bar charts shown on the right are the mean fluorescence intensity (MFI) of IL-15R α staining in IL-15R α -COS-7 cells which were untreated (orange bars), IL-15-treated (blue bars) or IL-15 Δ E7-treated (red bars) at indicated time after treatment. Background (shown in grey) was the fluorescence profile of untreated IL-15R α -COS-7 cells stained with isotype control antibody. (D) Results shown are percent reduction in MFI of IL-15R α staining in IL-15-treated or IL-15 Δ E7-treated at 0.5, 2, 4 and 6 hour compared with that in untreated IL-15R α -COS-7 cells. Formula: % of MFI reduction at i hour = $((\text{MFI of untreated cells at } i \text{ hour}) - (\text{MFI of IL-15-treated or IL-15}\Delta\text{E7 treated cells at } i \text{ hour})) / (\text{MFI of untreated cells at } i \text{ hour}) \times 100$, $i = 0.5, 2, 4$ and 6 . (E) Results shown are the rate of IL-15R α MFI reduction in untreated, IL-15-treated or IL-15 Δ E7-treated cells at indicated time interval. Formula: MFI reduction rate in the time interval $T = (\Delta\text{MFI in } T) / (\Delta\text{hour})$, $T_1 = 0\text{-}0.5$ hour, $T_2 = 0.5\text{-}2$ hour, $T_3 = 2\text{-}4$ hour and $T_4 = 4\text{-}6$ hour.

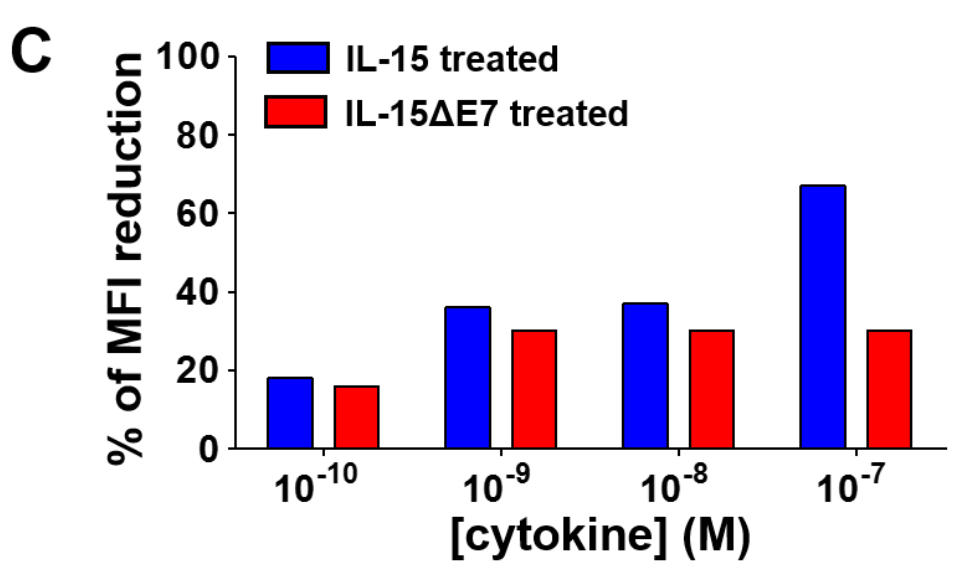
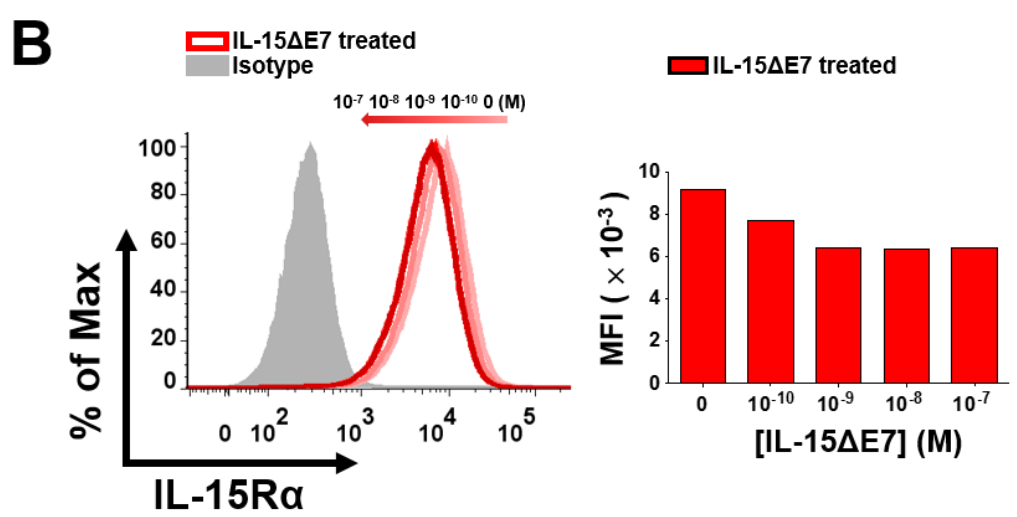
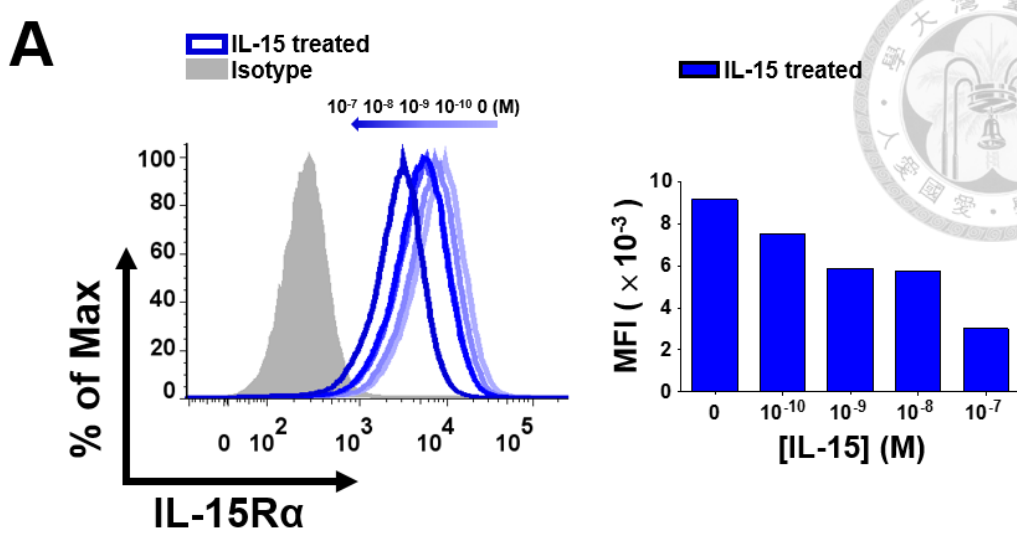


Figure 17. Surface expression of IL-15R α in IL-15R α -COS-7 cells after treated with IL-15 or IL-15 Δ E7 overnight

Dislodged IL-15R α -COS-7 cells (1.7×10^5 cells/mL) were treated with IL-15 or IL-15 Δ E7 at 10^{-7} , 10^{-8} , 10^{-9} or 10^{-10} M for 24 hours at 37°C in a 6-well microtiter plate (3mL/well). The cells were trypsinized and stained with goat anti-IL-15R α polyclonal antibody as described in the legend of Figure 15. GFP positive and propidium iodide negative cells were gated for live IL-15R α -COS-7 cells. Results shown are histogram profiles of IL-15R α staining in IL-15-treated (A) or IL-15 Δ E7-treated (B) IL-15R α -COS-7 cells at indicated concentration. (C) Results shown are percent of reduction in MFI of IL-15R α staining in IL-15-treated or IL-15 Δ E7-treated at 10^{-7} , 10^{-8} , 10^{-9} or 10^{-10} M compared with that in untreated IL-15R α -COS-7 cells. Formula: % of MFI reduction at [M] = $((\text{MFI of untreated cells at [M]}) - (\text{MFI of IL-15-treated or IL-15}\Delta\text{E7 treated cells at [M]})) / (\text{MFI of untreated cells at [M]}) \times 100$, [M] = 10^{-7} , 10^{-8} , 10^{-9} or 10^{-10} M. Background (shown in grey) was the fluorescence profile of untreated IL-15R α -COS-7 cells stained with isotype control antibody. Bar charts shown on the right are the mean fluorescence intensity (MFI) of IL-15R α staining in IL-15R α -COS-7 cells treated with various concentration of IL-15 (blue bars) or IL-15 Δ E7 (red bars) at each concentration.



Appendix

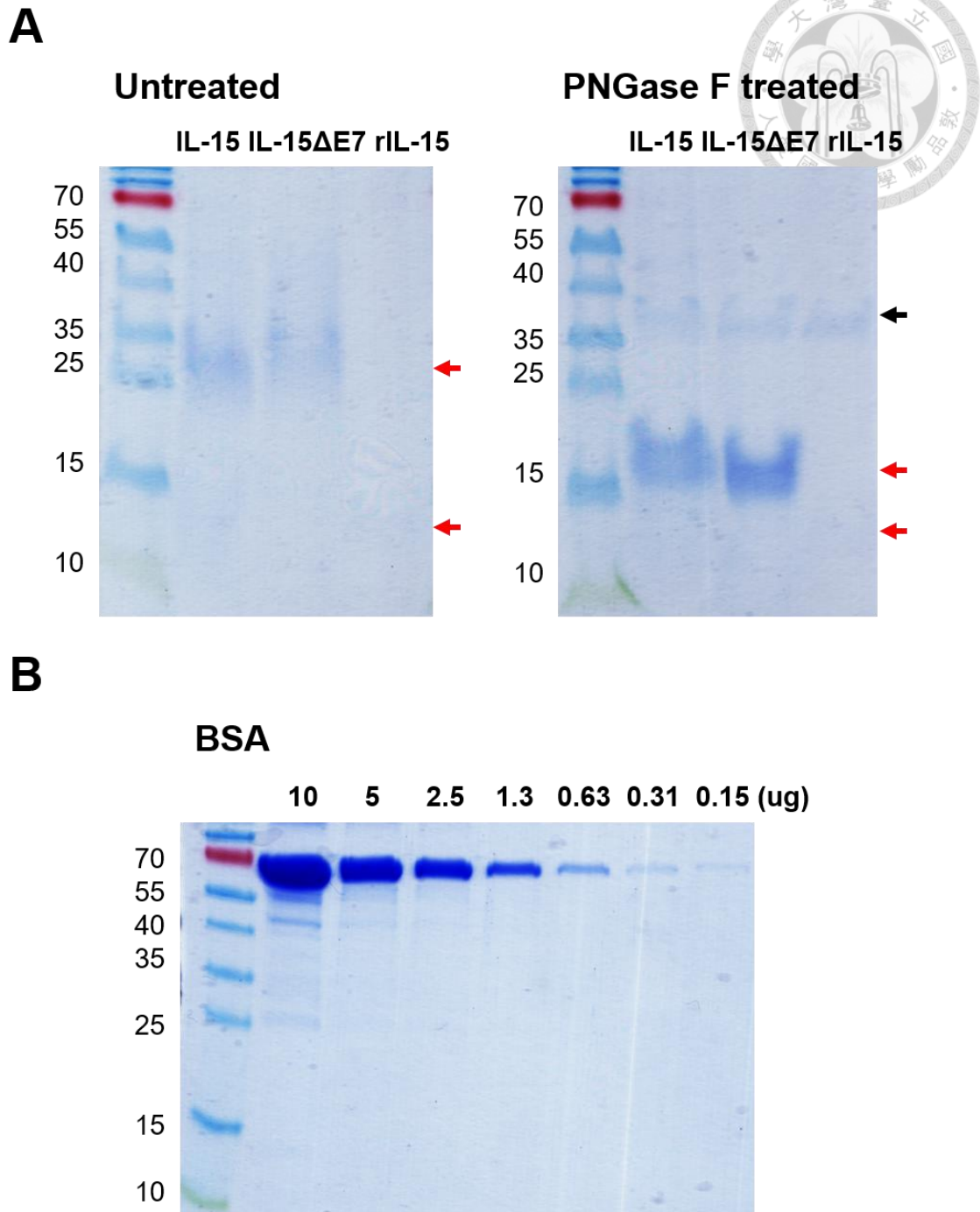


Figure A.1 Coomassie blue staining of IL-15 and IL-15ΔE7

10 ug of yeast recombinant IL-15 or IL-15ΔE7 or 1 ug of *E.coli* recombinant IL-15 left untreated or treated with PNGase F (A) or two-fold serially diluted BSA (B) was denatured in sample buffer with 1% β-mercaptoethanol and then resolved on a 15% SDS-PAGE by electrophoresis. Protein on the gel was then stained with Coomassie blue. The red arrows indicate yeast recombinant IL-15 or IL-15ΔE7 or *E.coli* recombinant IL-15. The black arrow indicates PNGase F.